Hindawi
Mediators of Inflammation
Volume 2023, Article ID 6699050, 31 pages
https://doi.org/10.1155/2023/6699050

Research Article

Integrative Analysis of Clinical and Bioinformatics Databases to Reveal the Role of Peripheral Innate Immunity in Kawasaki Disease

Hongjun Ba,[1,2] **Lili Zhang**,[1] **Huimin Peng**,[1] **Jixun Lin**,[1] **Youzhen Qin**,[1,2] **and Yao Wang**[3]

[1]*Department of Pediatric Cardiology, Heart Centre, The First Affiliated Hospital, Sun Yat-sen University, Guangzhou, China*
[2]*NHC Key Laboratory of Assisted Circulation and Vascular Diseases, Sun Yat-sen University, Guangzhou, China*
[3]*Guangzhou Medical University Cancer Hospital, Guangzhou, China*

Correspondence should be addressed to Yao Wang; wangyao@gzhmu.edu.cn

Received 14 July 2023; Revised 5 October 2023; Accepted 18 October 2023; Published 14 November 2023

Academic Editor: Cheorl-Ho Kim

Kawasaki disease (KD) is an immune-response disorder with unknown etiology. KD is an acute systemic immune vasculitis caused by infectious factors that can be complicated by coronary artery lesions. Innate immune cells are closely associated with KD onset, but we know little regarding the expression of immunity-related genes (IRGs) and the possible immune regulatory mechanisms involved in KD. In this study, we analyzed public single-cell RNA sequencing (scRNA-seq) and microarray data of peripheral blood mononuclear cells from normal controls and KD patients. The results of scRNA-seq revealed myeloid cells, T cells, B cells, NK cells, erythrocytes, platelets, plasma cells, hematopoietic stem cells, and progenitor cells in the peripheral blood of patients with KD. In particular, myeloid cells were expanded and heterogeneous. Further analysis of the myeloid cell population revealed that monocytes in KD exhibited higher expression of the inflammatory genes *S100A8*, *S100A9*, and *S100A12*; furthermore, CD14+CD16+ monocyte clusters were associated with inflammatory responses. Microarray data revealed that activation of the innate immune response contributed to KD development and progression. Differential expression and weighted gene coexpression network analysis identified 48 differentially expressed IRGs associated with response to intravenous immunoglobulin, currently the most effective treatment of KD, although numerous patients are resistant. Protein–protein interaction analysis identified ten hub genes (*IL1R1*, *SOCS3*, *IL1R2*, *TLR8*, *IL1RN*, *CCR1*, *IL1B*, *IL4R*, *IL10RB*, and *IFNGR1*) among the IRGs. In addition, the expressions of *IL1R1*, *SOCS3*, *CCR1*, *IL1B*, and *IL10RB* were validated in Chinese KD patients using the real-time reverse transcriptase-polymerase chain reaction. Finally, we found that the neutrophil/lymphocyte ratio could be used as a biomarker to predict responsiveness to intravenous immunoglobulin in KD. In conclusion, our data highlight the importance of innate immunity in KD pathogenesis and its potential in predicting treatment response.

1. Introduction

Kawasaki disease (KD), also known as cutaneous mucosal lymph node syndrome, was first reported from Japan in 1967 by Kawasaki [1]. KD is a disorder characterized by abnormal inflammation and an atypical immune response. Genetic factors, particularly variations in genes associated with the immune system, contribute to the risk of developing this condition [2]. Immune dysregulation and the activation of T cells and monocytes play a role in the disease [3, 4]. Inflammation and the formation of aneurysms in the coronary arteries are caused by dysfunction in the endothelial lining of blood vessels [5]. While the exact infectious agent responsible for KD remains unknown, some theories propose that specific viruses or bacteria may trigger the immune response [6]. However, the exact cause of KD remains unknown.

Immunohistochemical analysis of postmortem tissue from patients with KD has revealed the presence of monocytes, macrophages, and neutrophils [3, 4], as well as activated

Table 1: Enrolled datasets in the current study.

Datasets	Type	Platform	Sample size (Control/KD)	Cells (Control/KD)	Reference
GSE168732	scRNA sequencing	GLP18753 Illumina NextSeq 500 (*Homo sapiens*)	6/3	24,679/14,033	[11]
GSE152450	scRNA sequencing	GPL24676 Illumina NovaSeq6000 (*Homo sapiens*)	2/2	3,981/2,302	[13]
GSE18606	RNA microarray	GPL8328 SMD Print-853	20/9	–	[19]
GSE63881	RNA microarray	GPL10558 Illumina human HT-12 V4.0 expression beadchip	171/170	–	[20]

$CD8^+$ T cells [7] and IgA^+ plasma cells [8, 9], in the arterial wall. Infiltrating immune cells release proinflammatory cytokines (e.g., TNF and IL-1β) that then contribute to the development of endothelial lesions and CAL [10, 11]. In addition, endothelin autoantibodies can cause endothelial disease in KD [12]. Recent research using single-cell RNA sequencing (scRNA-seq) has revealed alterations to immune cells in KD patients at the acute stage, including increases in immunomodulatory T cells, NK cells [13], plasma cells, and B cells [14]. Immunomodulatory genes are involved in the pathogenesis of KD [15]. Changes have also been observed in monocyte developmental trajectory [16], and CD14+CD16- monocytes were found to be expanded in KD. Multisystem Inflammatory Syndrome in Children (MIS-C), an inflammatory disorder associated with immune dysfunction, has clinical manifestations similar to KD which are sometimes difficult to distinguish. Immunological studies showed a decrease in the number of follicular B cells, an increase in the number of terminally differentiated CD4+T lymphocytes (LYM), and a decrease in IL-17A levels in MIS-C [17]. These studies suggest that innate immunity plays an important role in KD pathogenesis. Furthermore, the most effective treatment for KD is currently high-dose intravenous gamma globulin (IVIG), which reduces CAL incidence. However, up to 15%–20% of patients do not respond to IVIG therapy, and CAL progression remains unaffected [17, 18]. An improved understanding of the mechanisms underlying the involvement of innate immunity could help to explain the nonresponsive patients. One promising area of research is immunity-related genes (IRGs), known to be critical during immune infiltration [19, 20]. No research has yet examined their regulation or expression characteristics in KD.

The objective of our study was to explore the role of innate immunity in the pathogenesis of KD and its potential in predicting treatment response. Here, we used scRNA-seq and RNA microarray data to investigate the expression characteristics of IRGs and their possible regulatory mechanisms. Furthermore, we validated the hub genes in Chinese KD patients. We demonstrated that $CD14^+CD16^+$ monocytes are important effector cells in the acute stage of KD, and regulate cytokine levels through promoting the expression of inflammatory transcription factors. Moreover, $CD14^+CD16^+$ and $CD14^-CD16^+$ monocytes are closely related to the efficacy of IVIG treatment. Our findings provide insight into the role of innate immunity in KD pathogenesis and offer valuable biomarkers that can be useful for improving treatment efficacy.

2. Materials and Methods

2.1. Gene Expression Datasets. Two whole-blood RNA microarray datasets (GSE18606 [21] and GSE63881 [22]) and two scRNA-seq datasets (GSE168732 [14] and GSE152450 [16]) were obtained from the Gene Expression Omnibus (GEO) database (https://www.ncbi.nlm.nih.gov/geo/) (Table 1). GSE63881 array data included acute and convalescent whole blood transcriptional profiles of 171 KD patients before IVIG administration (110 IVIG responders and 61 nonresponders). GSE18606 comprised expression profiles of nine healthy age-appropriate subjects and 20 acute KD subjects (8 nonresponders and 12 responders). Whole blood peripheral blood mononuclear cells (PBMC) were used for scRNA-seq; GSE168732 data contained six KD and three healthy subjects. Analysis of GSE152450 data revealed monocyte heterogeneity in two healthy and two KD infants.

2.2. Analysis of scRNA Sequencing Data. Processing of GSE168732 scRNA sequencing data followed methods from a previous study [14]. The quality control standards are as follows: first, we assigned the CreateSeuratObject function various parameters, including min. Cell = 3 and min. features = 200. For most samples, the total UMI count is between 2,000 and 60,000, and the mitochondrial gene percentage was <5%. For P1 before therapy, a lower cutoff of total UMI count (1,000) was used owing to its lower median UMI count per cell. After quality control and filtering, 38,712 cells were selected for the analysis. Processing of the GSE152450 dataset also followed published methods [16], yielding 6,283 cells for further analysis after quality control and filtering. The "Findmarkers" function of the R package *Seurat* [23] was used to perform downstream analyses of differentially expressed genes (DEGs). Criteria for DEGs were adjusted $P < 0.05$ and $|\log \text{fold change}| \geq 0.25$. R packages *Monocle2* [24] and *Dorothea* [25] were used to determine the pseudo-time developmental trajectory and transcription factor activity of myeloid subpopulations, respectively.

2.3. Score Analysis of IRGs. IRGs were downloaded from ImmPort (https://www.immport.org/shared/home) [26]. The R package *AUCell* was used to calculate IRG scores among cell clusters, following publicly available code and tutorial (https://www.bioconductor.org/packages/devel/bioc/vignettes/AUCell/inst/doc/AUCell.html).

Table 2: Primers used for RT-qPCR with their sequence.

Gene	Forward primer (5′–3′)	Reverse primer (5′–3′)
IL1R1	CGTCCCTGTCCTCTTAACCCAAATG	TGTGTTGATGAATCCTGGAGGCTTG
SOCS3	GACTGCGTGCTCAAGCTGGTG	CTCGGAGGAGGGTTCAGTAGGTG
IL1R2	GACGGTGCTCTGTGGCTTCTG	GGGTATGAGATGAACGGCAGGAAAG
TLR8	GGAGCCAGTGTTACAGCATTCTCAG	GCCTTCTGCCTTCGGGTTGTC
IL1RN	GTGCCTGTCCTGTGTCAAGTCTG	GCCACTGTCTGAGCGGATGAAG
CCR1	CAACTCCGTGCCAGAAGGTGAAC	AAGGACCAGGACCACCAGGATG
IL1B	GGACAGGATATGGAGCAACAAGTGG	TCATCTTTCAACACGCAGGACAGG
IL4R	AGGAGGAGGAGGAGGTAGAGGAAG	TCCGAGCAGGTCCAGGAACAG
IL10RB	GAGCAAACAACCCATGACGAAACG	CACCACAGCAAGGCGAAGCAG
IFNGR1	AGATTCAGTGCCAGTTAGCGATTCC	CCCACACATGTAAGACTCCTTCTGC

2.4. Microarray Data Analysis. The R package immunooncology biological research [27] was used to construct the expression matrix and to match the probes with gene symbols. Downstream analysis, including normalization and analysis of DEGs (adjusted $P < 0.05$, and $|\log \text{fold change}| \geq 1.0$), was done with R package *limma* [28].

2.5. Weighted Gene Coexpression Network Analysis. Gene coexpression networks were constructed with the R package weighted gene coexpression network analysis (*WGCNA*) [29]. After analyzing the correlation modules and different sample periods, MEblue modules were selected for further analysis because they had the highest positive correlation with responders from acute samples. The code and tutorial were obtained online (https://rstudio-pubs-static.s3.amazonaws.com/687551_ed469310d8ea4652991a2e850b0018de.html).

2.6. Functional Analysis. Gene Ontology (GO) and Kyoto Encyclopedia of Genes and Genomes (KEGG) analyses were performed for DEGs using clusterProfiler [30]. Differences were considered significant at adjusted $P < 0.05$. The R package *GSVA* (gene set variation analysis) was applied on hallmark gene sets among cell clusters [31].

2.7. Protein–Protein Interaction Analysis and Validation of Hub Genes. Network analysis of protein–protein interactions (PPIs) was performed using STRING (https://string-db.org/) [32]. Hub genes were identified in Cytoscape version 3.8.2. Real-time reverse transcriptase-polymerase chain reaction (RT-qPCR) assays were performed to verify the reliability of bioinformatics-based results. A total of 28 study participants were recruited from the First Affiliated Hospital of Sun Yat-sen University, including 18 KD patients (10 IVIG-responsive, 8 IVIG-nonresponsive), and 10 healthy controls. The protocol was approved by the Ethics Committee of the First Affiliated Hospital of Sun Yat-sen University ((2022)514). Peripheral venous blood was collected from each participant; then, total RNA was extracted from each sample using TRIzol (Invitrogen, United States) according to the manufacturer's instructions. The cDNA was synthesized using the SuperScript III Reverse Transcriptase Kit (Invitrogen, USA). RT-qPCR was performed with Power SYBR Green PCR Master Mix (TransGen Biotech, China) on an ABI 7500 fast real-time PCR system. The amplification reaction procedure was as follows: 95°C for 10 min, followed by 95°C for 15 s and 60°C for 1 min for 40 cycles. *GAPDH* was selected as the internal control for mRNA, and the relative expression level of mRNA was calculated by the relative quantification ($2^{-\Delta\Delta Ct}$) method. The primer sequences are listed in Table 2.

2.8. Laboratory Indicators of KD. Clinical data and common laboratory inflammation indices were collected from patients diagnosed with KD between January 2014 and January 2021 in the Department of Pediatric Cardiology at the First Affiliated Hospital of Sun Yat-sen University. The nature and purpose of the study was carefully explained to parents before written consent was obtained from the parents. The protocol was approved by the Ethics Committee of the First Affiliated Hospital of Sun Yat-sen University ((2022)514). All patients had acute KD. Individuals were excluded if they had other systemic diseases (e.g., kidney disease), or did not receive IVIG. The diagnostic criteria for KD were based on literature [33]. Patients were divided into IVIG-responsive and IVIG-resistant groups [33]. Inflammatory markers, including C-reactive protein (CRP), procalcitonin (PCT), white blood cells, neutrophils (NEUT), LYM, monocytes (MONO), and platelets (PLT) were collected; the neutrophil/lymphocyte ratio (NLR) was then calculated. These indicators were measured before IVIG administration.

2.9. Statistical Analysis. Wilcoxon tests or Kruskal–Wallis tests were used for between-group comparisons. All statistics and visualizations used R and the *ggplot2* package [34]. Results from descriptive analyses are reported as percentages and medians (interquartile spacing), as appropriate. Significance was set at $P < 0.05$.

3. Results

3.1. Profiling of scRNAs from KD PBMCs. Analysis of GSE168732 involved 36,849 cells (22,775 KD patients and 14,074 normal controls (NC)). After filtration, we retained 24,679 cells (14,033 patients with KD and 10,646 NC). The expression characteristics of each sample are shown in Figure S1.

Cells were assigned to known clusters based on marker genes [11]. Using t-SNE analysis, we visualized nine clusters: myeloid cells, T cells, B cells, NK cells, erythrocytes, platelets,

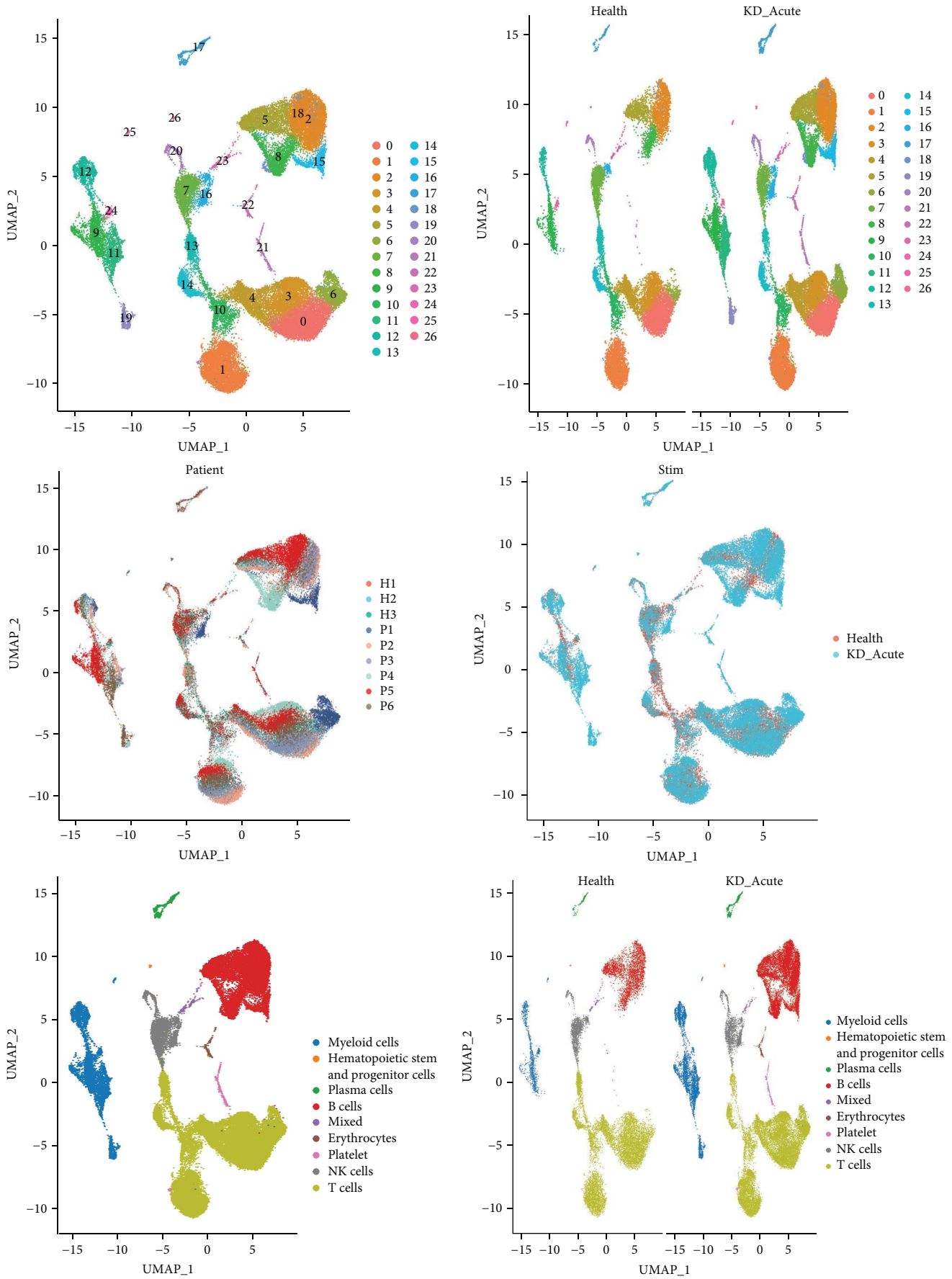

(a)

Figure 1: Continued.

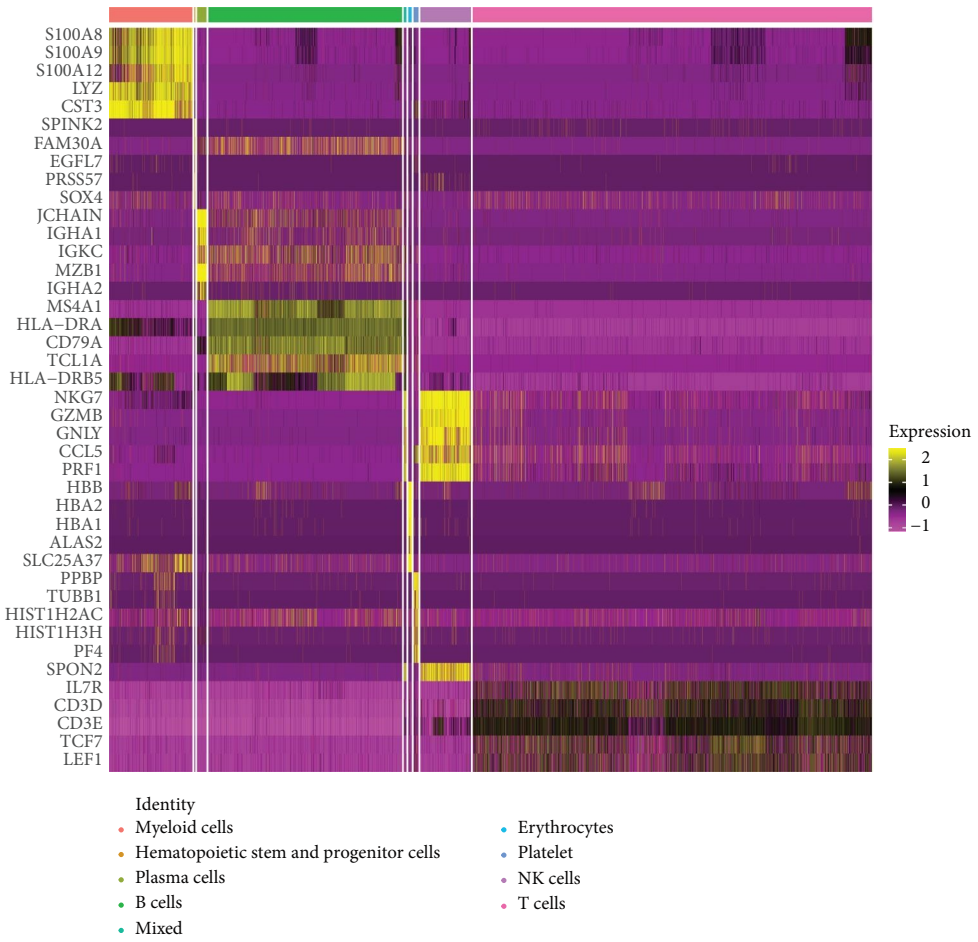

(b)

Figure 1: Continued.

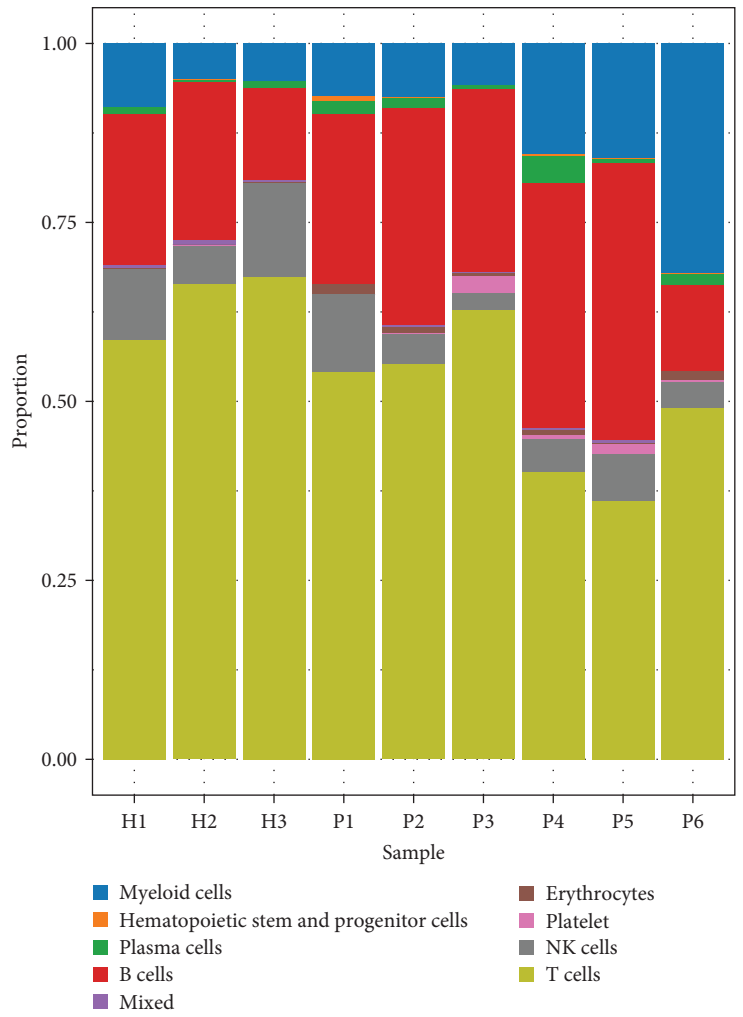

(c)

Figure 1: Continued.

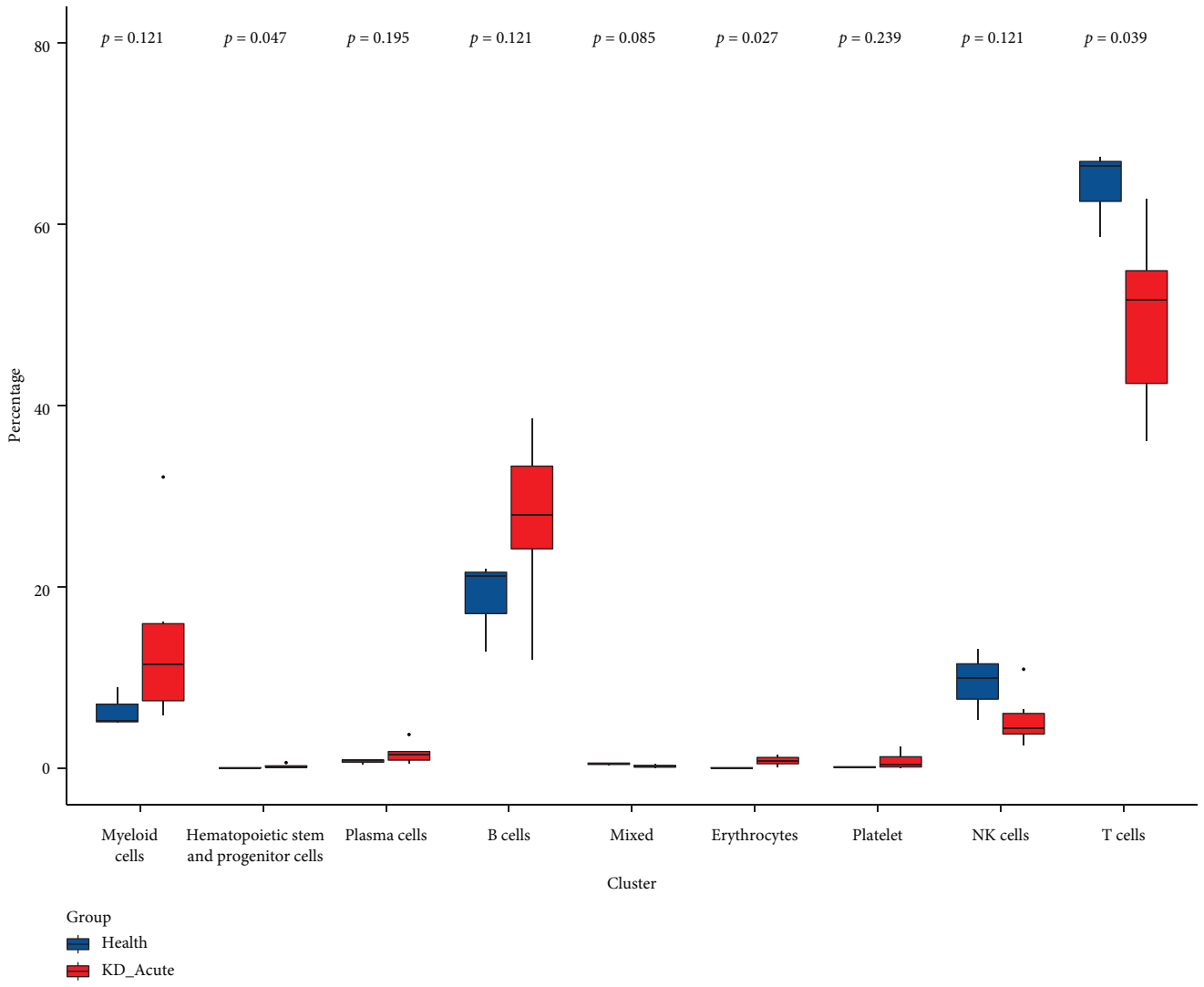

Figure 1: Cluster distribution analysis. (a) Cell types identified in peripheral blood mononuclear cells (PBMC) using uniform manifold approximation and projection (UMAP). (b) Cluster heat map of top five differentially expressed genes (DEGs) per cluster. (c) Cluster distribution in each sample. (d) Cluster distribution in Kawasaki disease (KD) and normal control (NC) groups. $^{*}P<0.05$.

plasma cells, hematopoietic stem cells, and progenitor cells, and mixed clusters (Figure 1(a) and Table S1, for all marker gene expression, see Figure S2). The KD group exhibited an increase in the number of myeloid and B cells (Figure 1(a)). We then identified DEGs (between KD and NC groups) in each cell cluster (the top five DEGs per cluster are shown in Figure 1(b)).

Compared with the NC group, T cells in the KD group decreased significantly, while myeloid cells increased, but not significantly (Figures 1(c) and 1(d) and Table 3).

3.2. Expression of IRG in PBMC Clusters from KD Patients. We selected IRGs according to the import database, and then obtained them from DEGs of each cluster in the PBMCs, resulting in 381 IRGs for analysis (Table S2).

The uniform manifold approximation and projection analysis revealed that myeloid cells had the highest number of DEGs among the nine cell subgroups (Figure 2(a)). We confirmed this outcome with area under the curve (AUC) analyses of IRG activity, where cells expressing more genes had higher AUC values (Figures 2(b) and 2(c)). Next, GO and KEGG analyses of 381 IRGs revealed that they were mainly enriched in immune response-activating cell surface receptor signaling pathway and cytokine–cytokine receptor interaction (Figures 2(d) and 2(e)). These data suggest that myeloid cell clusters are heterogeneous and that the innate immune system plays an essential role in the development of KD. Therefore, we mainly focused on myeloid cells in subsequent analyses.

3.3. Characteristics of Monocyte Expression in KD. Further reclustering analysis of myeloid cells based on cell-type marker genes showed that the main components were $CD14^{+}CD16^{+}$ monocytes, leukocyte immunoglobulin-like receptor $A4^{+}$ plasmacytoid dendritic cells ($LILRA4^{+}$ pDC), $CD14^{+}CD16^{-}$ monocytes, and $CD14^{-}CD16^{+}$ monocytes

Table 3: Cell numbers of each cluster.

Cluster	Myeloid cells	B cells	T cells	NK cells	Erythrocytes	Platelet	Plasma cells	Mixed	Hematopoietic stem and progenitor cells
KD1	303	965	2,203	443	57	0	76	3	24
KD2	381	1,530	2,783	214	41	7	70	17	4
KD3	303	1,347	3,294	129	20	124	25	6	6
KD4	746	1,658	1,940	220	36	23	179	14	14
KD5	1,272	3,049	2,851	514	5	119	52	42	4
KD6	1,066	397	1,628	121	43	7	52	1	4
NC1	467	1,113	3,081	519	1	3	46	27	4
NC2	220	966	2,907	231	0	10	17	28	2
NC3	263	649	3,389	657	3	2	47	17	1

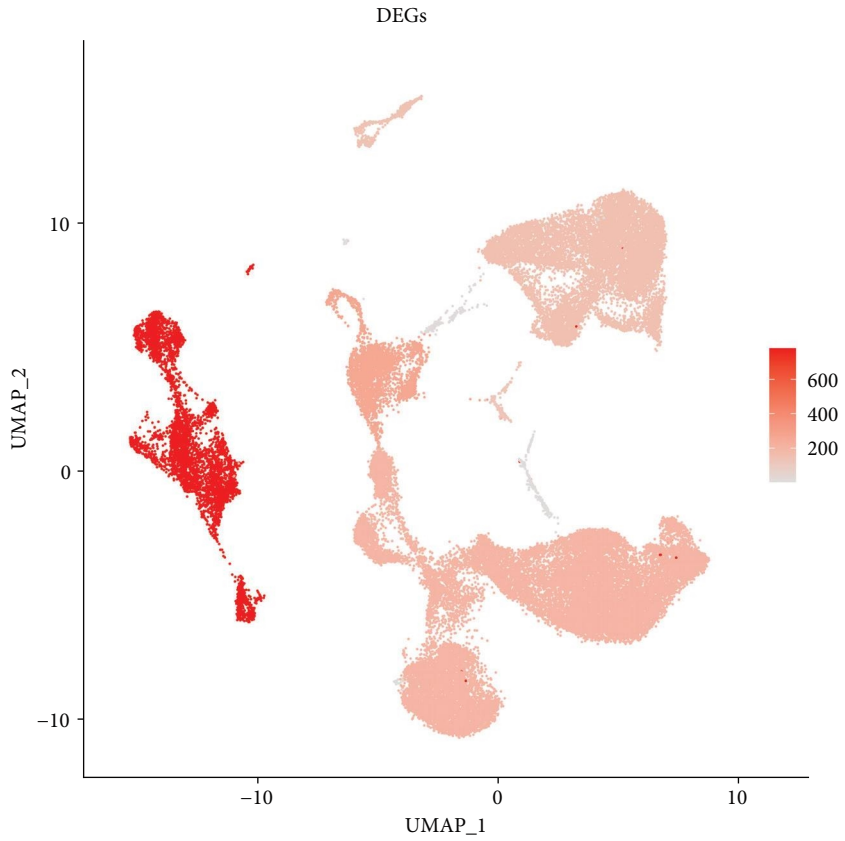

(a)

Figure 2: Continued.

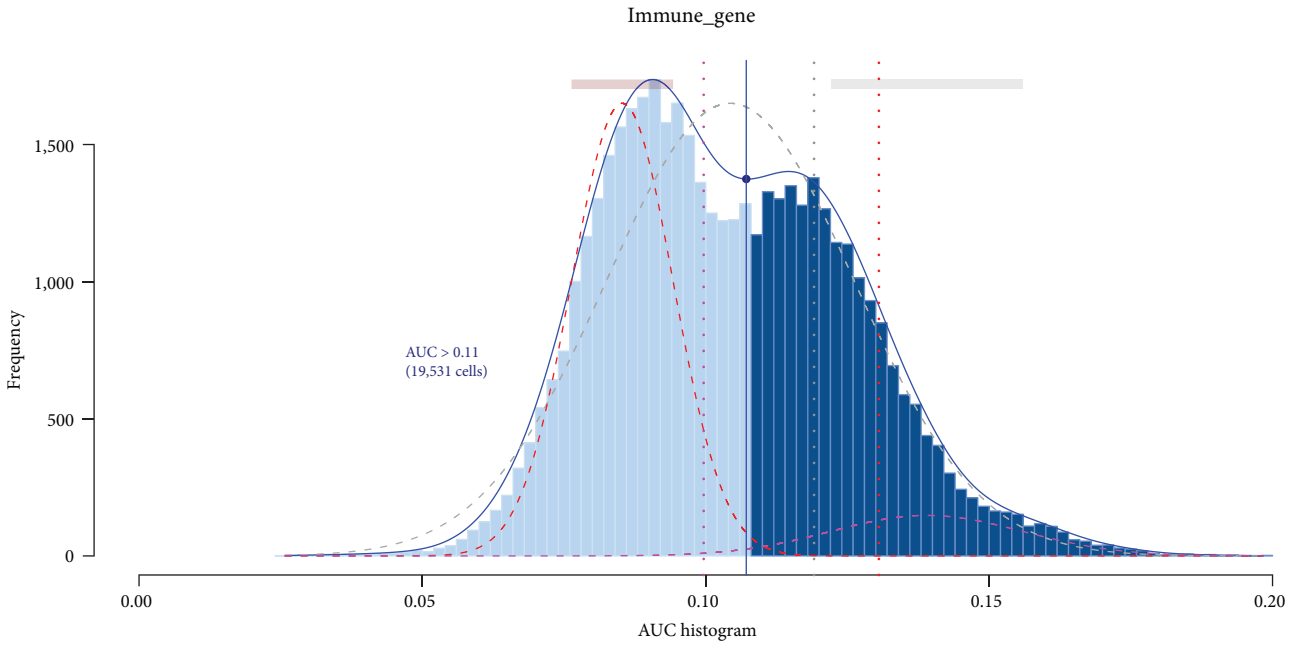

(b)

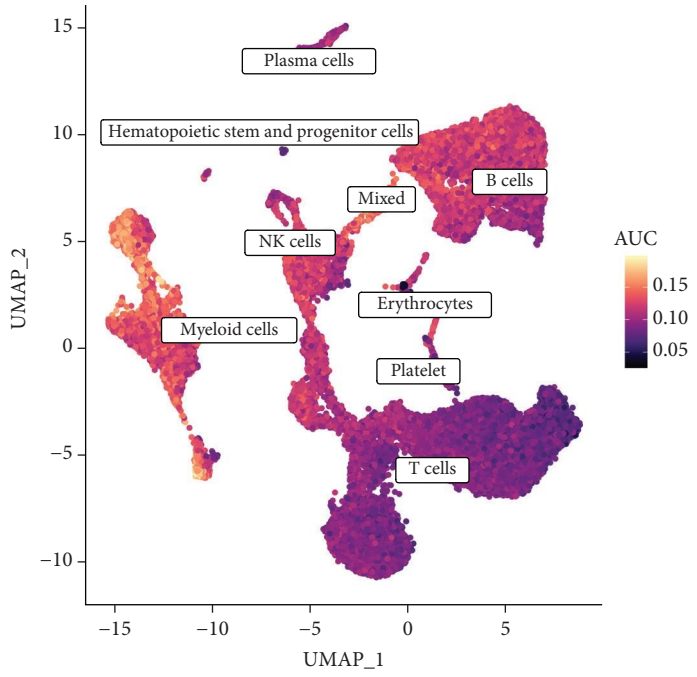

(c)

Figure 2: Continued.

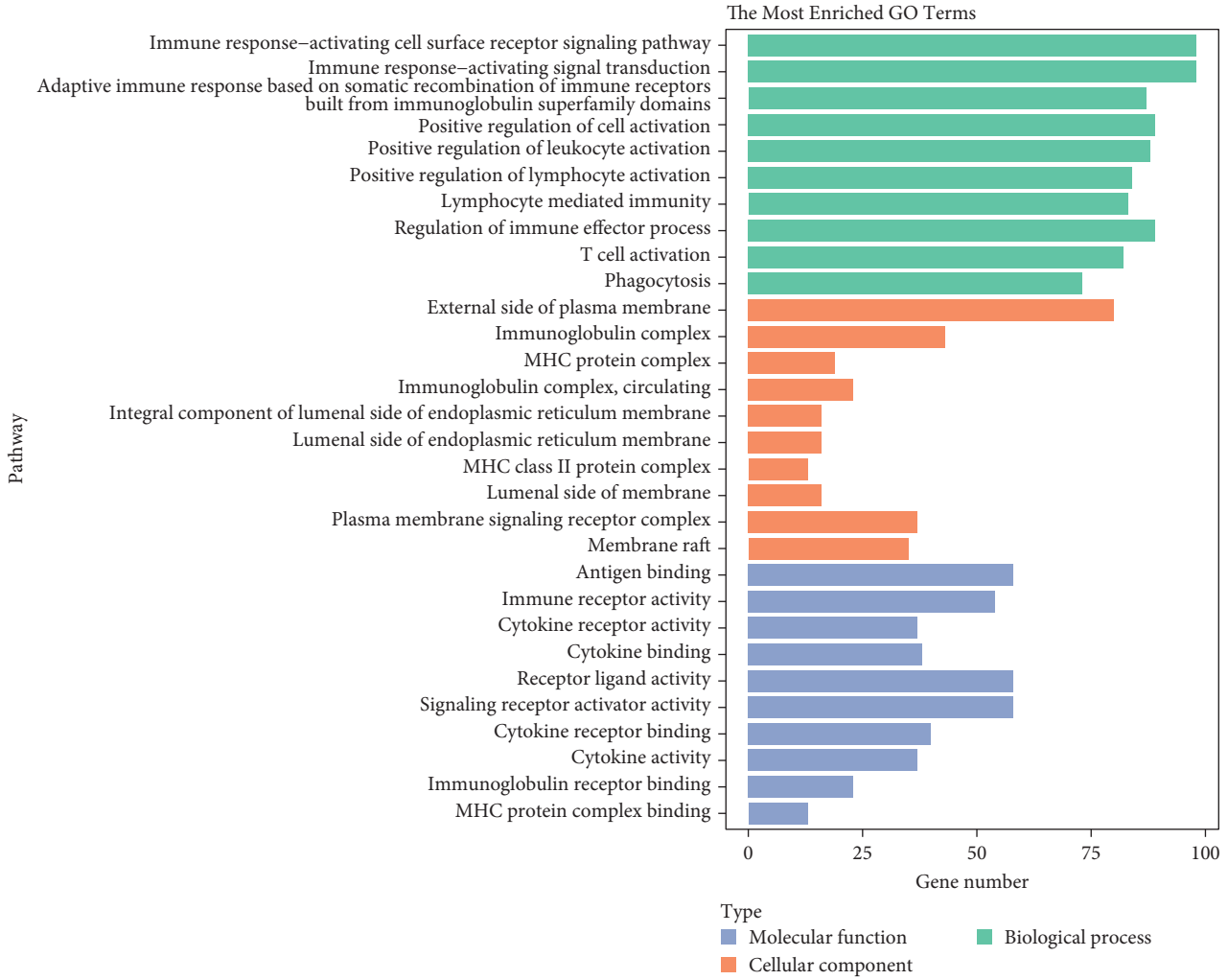

(d)

Figure 2: Continued.

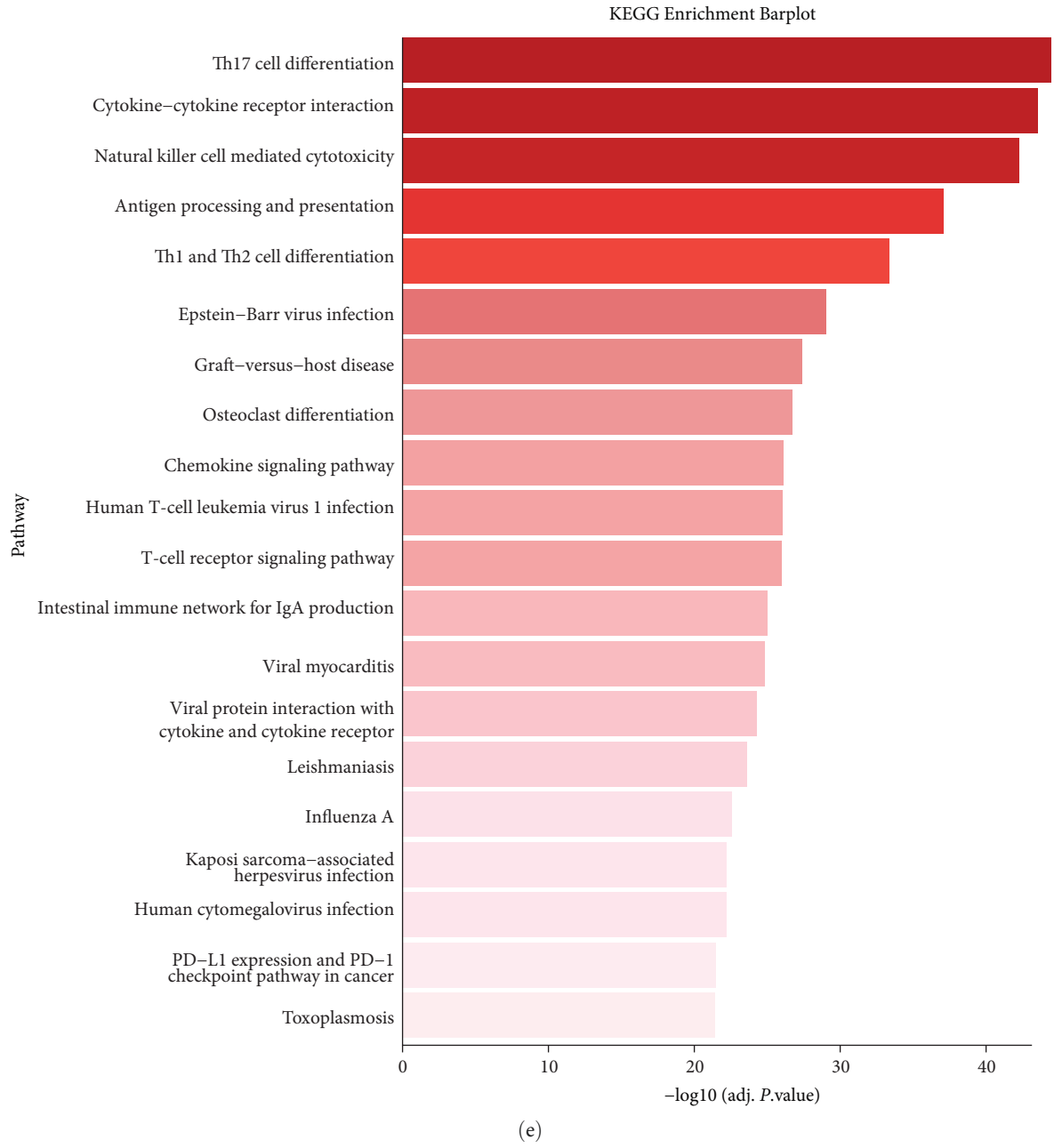

(e)

FIGURE 2: Immunity-related gene (IRG) scores of PBMC clusters in KD. (a) DEGs in cell clusters from KD samples. Myeloid cells had the most DEGs. (b) Scores of 381 screened IRGs. The threshold was 0.11. (c) t-SNE plots of IRG scores in all clusters. Myeloid cells express more genes and exhibit higher AUC values. (d) Gene Ontology (GO) analysis of DEGs in myeloid cells, revealing enrichment in immune response-activated cell surface receptor signaling pathway and immune response-activated signal transduction. (e) KEGG analysis of DEGs in myeloid cells, revealing enrichment in pathways associated with Th17 cell differentiation, cytokine–cytokine receptor interaction, and natural killer cell-mediated cytotoxicity.

(Figure 3(a) and Figure S3). A previous study reported that peripheral blood monocytes play a central role in acute KD [35]. We thus compared monocyte expression between the KD and NC groups, revealing that monocytes in the KD group expressed the calgranulin genes *S100A8*, *S100A9*, and *S100A12* at significantly higher levels (Figure 3(b)). Dot plots showed that these inflammatory genes were mainly concentrated in $CD14^{+}CD16^{+}$ monocytes (Figure 3(c)). Pseudotime analysis of monocyte subsets indicated that the developmental trajectory started from $CD14^{-}CD16^{+}$ monocytes and ended with $CD14^{+}CD16^{+}$ monocytes; additionally, inflammatory gene expression increased during development (Figure 3(d)). Next, GSVA of significant hallmarks in myeloid cells indicated that immunomodulatory genes associated with the inflammatory response were significantly upregulated in $CD14^{+}CD16^{+}$ monocytes from the KD group (Figure 4(a)). A

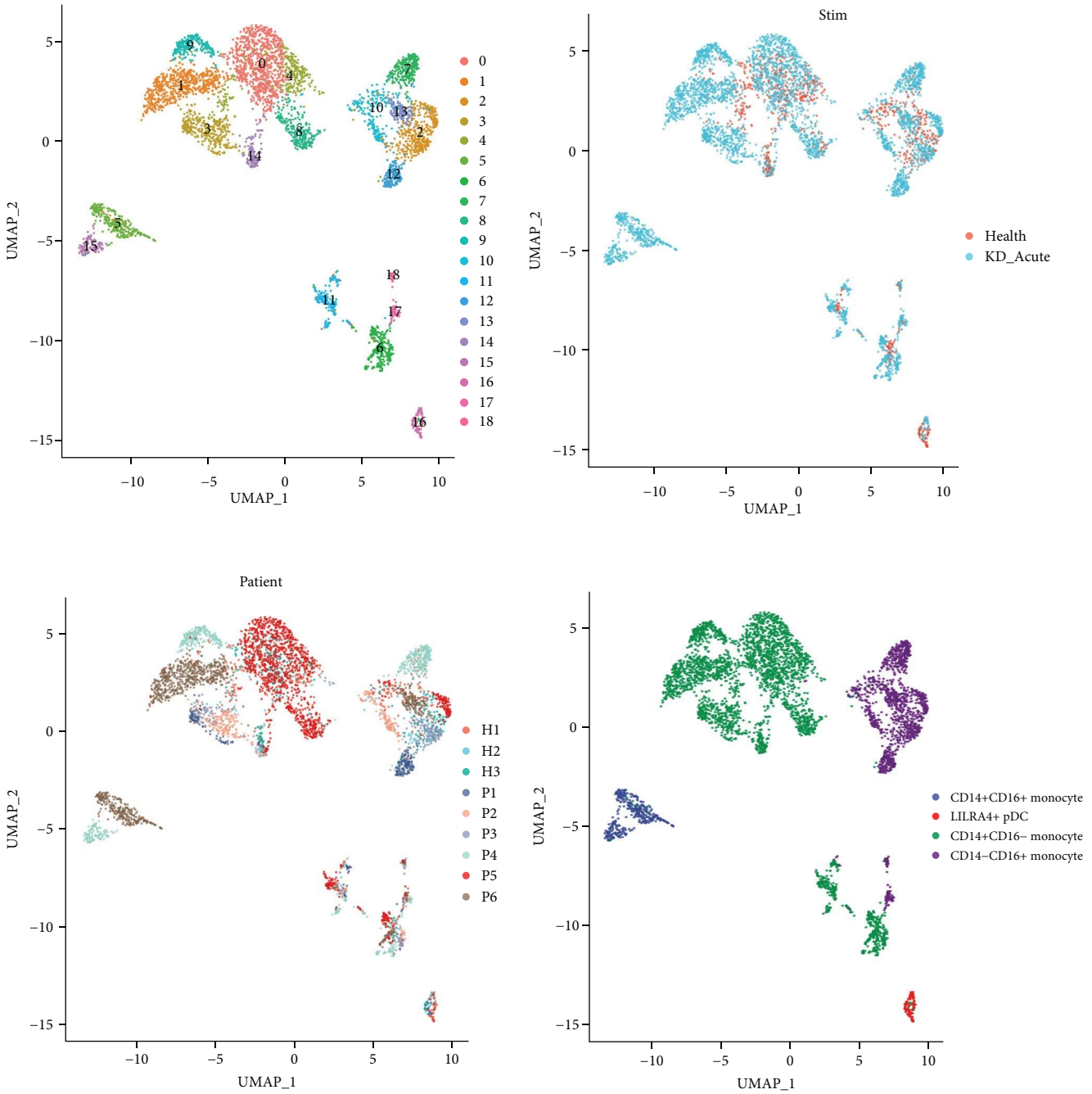

(a)

Figure 3: Continued.

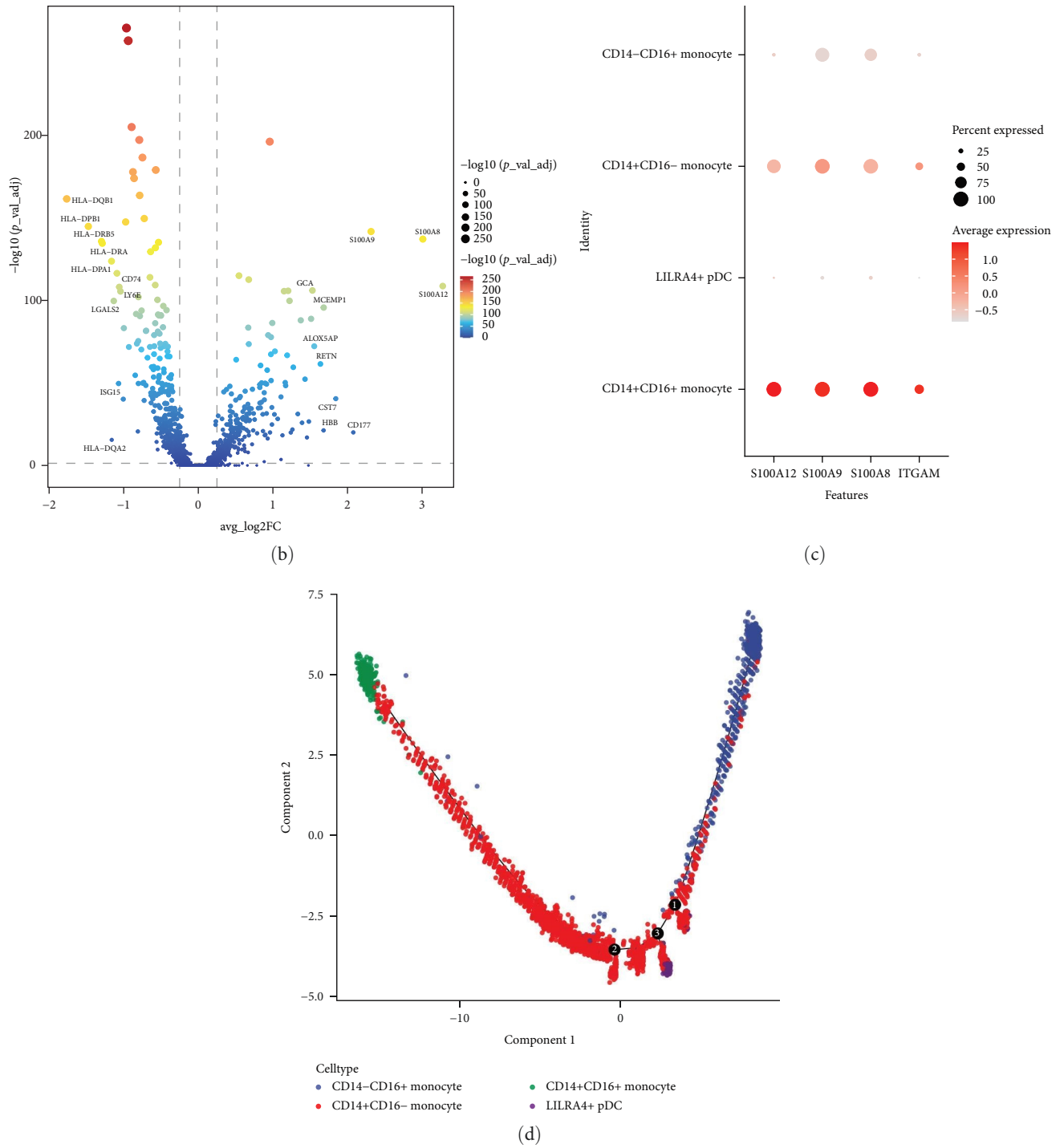

FIGURE 3: Analysis of myeloid cell subsets. (a) Cell types identified in myeloid cells using UMAP. (b) Volcano plot of DEGs ($|\log FC| \geq 0.25$ and adjusted $P < 0.05$). The top 20 DEGs are marked. (c) Expression of four major DEGs in myeloid cells. The dot size represents the percent expressed, and the color scale represents the average expression. The DEGs were mainly expressed in $CD14^{+}CD16^{+}$ monocytes. (d) Pseudotime analysis of monocyte subsets in KD, using Monocle. The developmental trajectory began with $CD14^{-}CD16^{+}$ monocytes and ended with $CD14^{+}CD16^{+}$ monocytes; inflammatory gene expression increased during development.

heat map showing functional enrichment indicated that transcription factors related to inflammatory NFKB1 were highly expressed in $CD14^{+}CD16^{+}$ monocytes, suggesting their likely involvement in the inflammatory response of KD (Figure 4(b)).

3.4. Differentially Expressed Genes in RNA Microarray Data of KD. We analyzed the RNA microarray dataset GSE18606 containing 12 IVIG-responsive KD patients and nine controls to explore DEGs in KD and screen for common IRGs in myeloid cells. We identified 5,339 up- and 5,542 downregulated

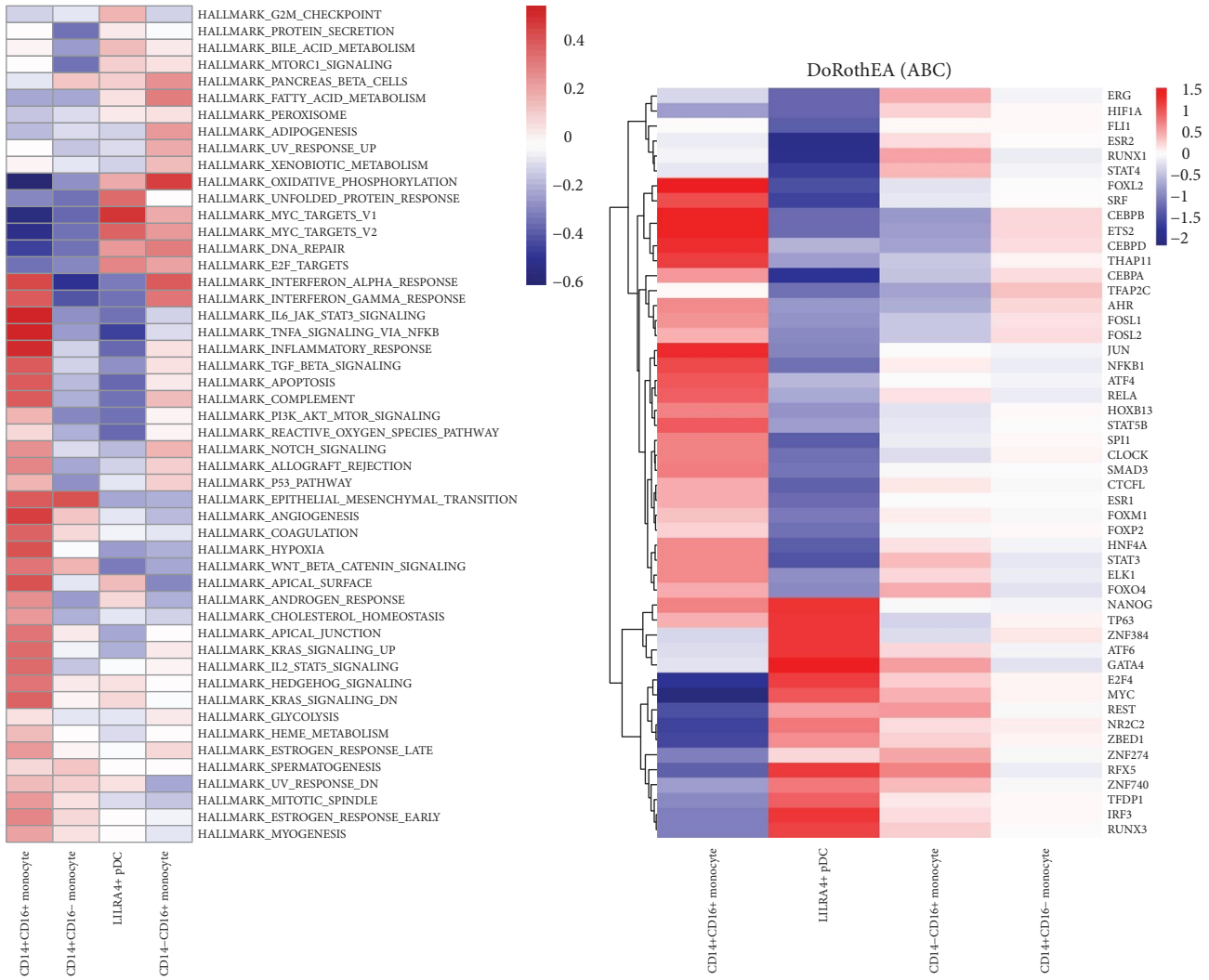

Figure 4: Functional enrichment analysis of DEGs in myeloid cells. (a) Gene set variation analysis (GSVA) in myeloid cell subsets. $CD14^+CD16^+$ monocytes were the most abundant cells with DEGs related to inflammatory signaling pathways. (b) Heat map of transcription factors with functional enrichment in monocytes and $LILR4^+$pDC cells. CD14+CD16+ monocytes have the most immunomodulatory transcription factors.

DEGs in KD (Table S3), including the inflammatory genes *S100A8* and *S100A12* (Figure 5(a)). Among these DEGs, we found 289 IRGs in the KD group (Figure 5(b)). According to GO analysis, these IRGs were enriched in pathways related to innate immunity, including neutrophil chemotaxis and myeloid leukocyte migration. (Figure 5(c)). Moreover, t-SNE plots of IRG scores in all clusters indicated that the 289 IRGs were mainly expressed in members of the innate immunity myeloid cell cluster (Figures 5(d) and 5(e)). These results further indicate that innate immunity is associated with KD pathogenesis.

3.5. Confirmation of Monocyte Function in KD. We used the scRNA sequencing dataset GSE152450 to confirm monocyte infiltration into KD. We grouped 2,302 myeloid cells into five subsets, including $CD14^+16^+$ monocytes, $CD14^+CD16^-$ monocytes, $CD14^-CD16^+$ monocytes, $CD1C^+$ classical dendritic cells, and $LILR4^+$ pDC cells; monocytes were dominant (Figures 6(a) and 6(b)). Analysis of DEGs in monocytes between KD and NC groups showed that *S1008A*, *S1009A*, and other inflammatory regulatory genes were highly expressed in KD (Figure 6(c)). Again, GSVA of hallmarks indicated that monocytes were primarily involved in inflammatory processes (Figure 6(d)). In summary, GSE152450 analysis confirmed that monocytes are closely related to the inflammatory response in KD.

3.6. Identification of Hub Genes Related to IVIG-Responsive Acute KD. To investigate biomarkers of IVIG-responsive acute KD, we analyzed whole blood RNA microarray data from patients with IVIG-resistant and IVIG-responsive KD. The results of WGCNA analysis (GSE63881) showed that IVIG-responsive KD had a highly synergistic gene set that correlated with disease phenotype (Figures 7(a) and 7(b)). These hub

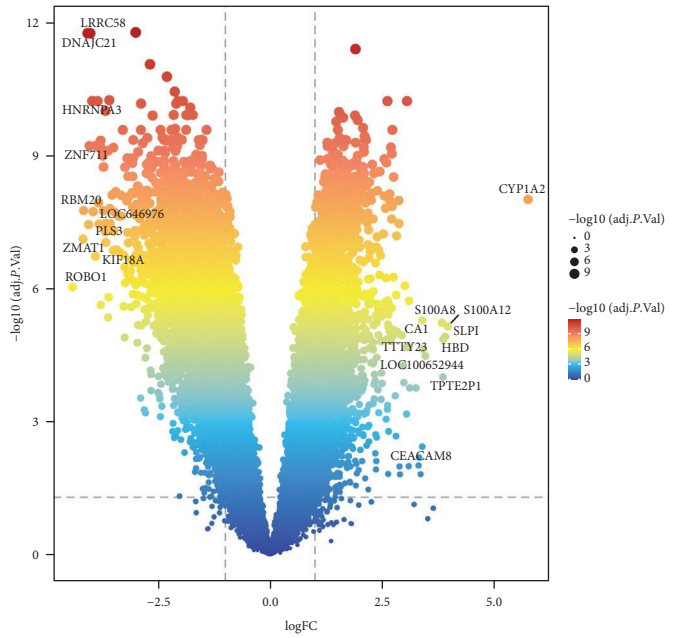

(a)

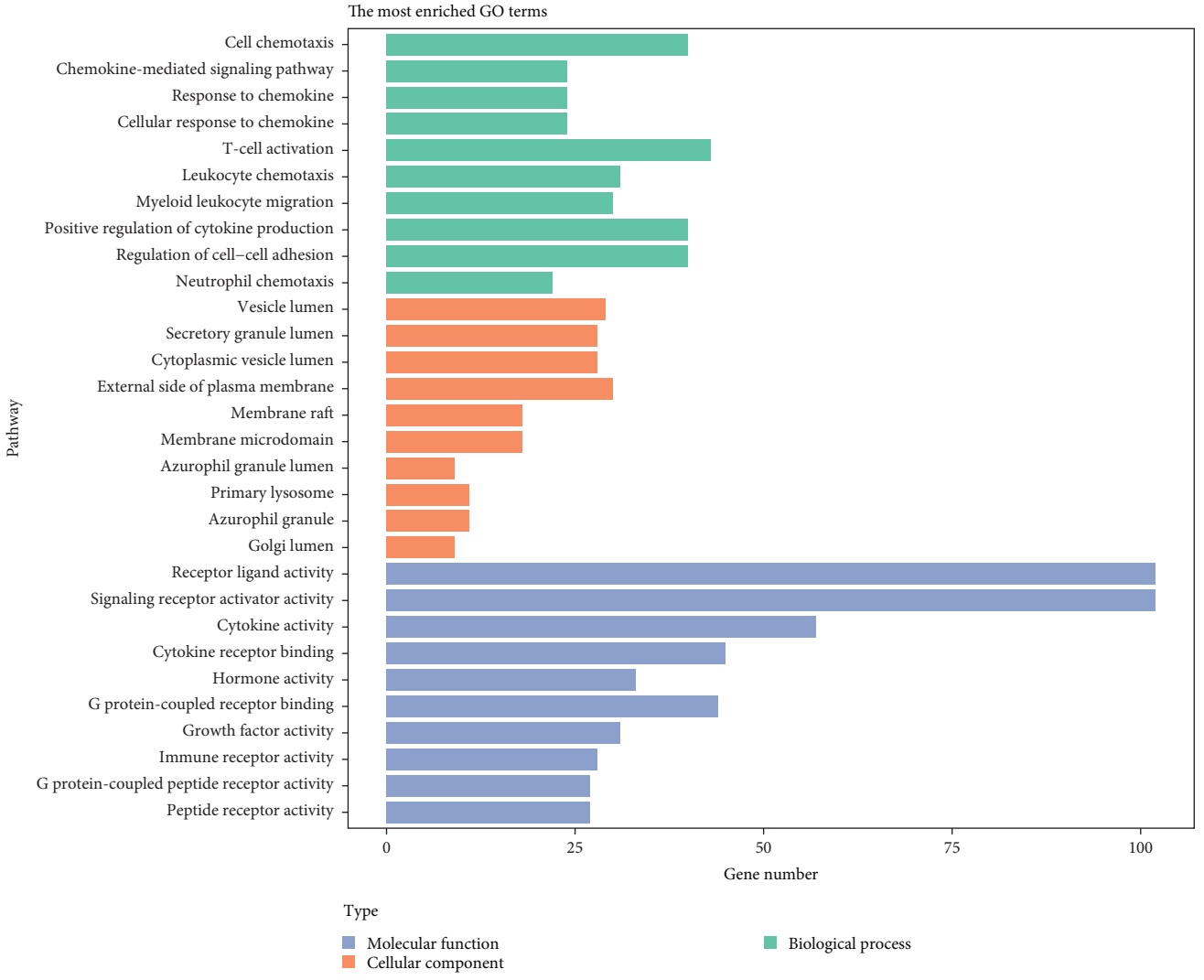

(b)

Figure 5: Continued.

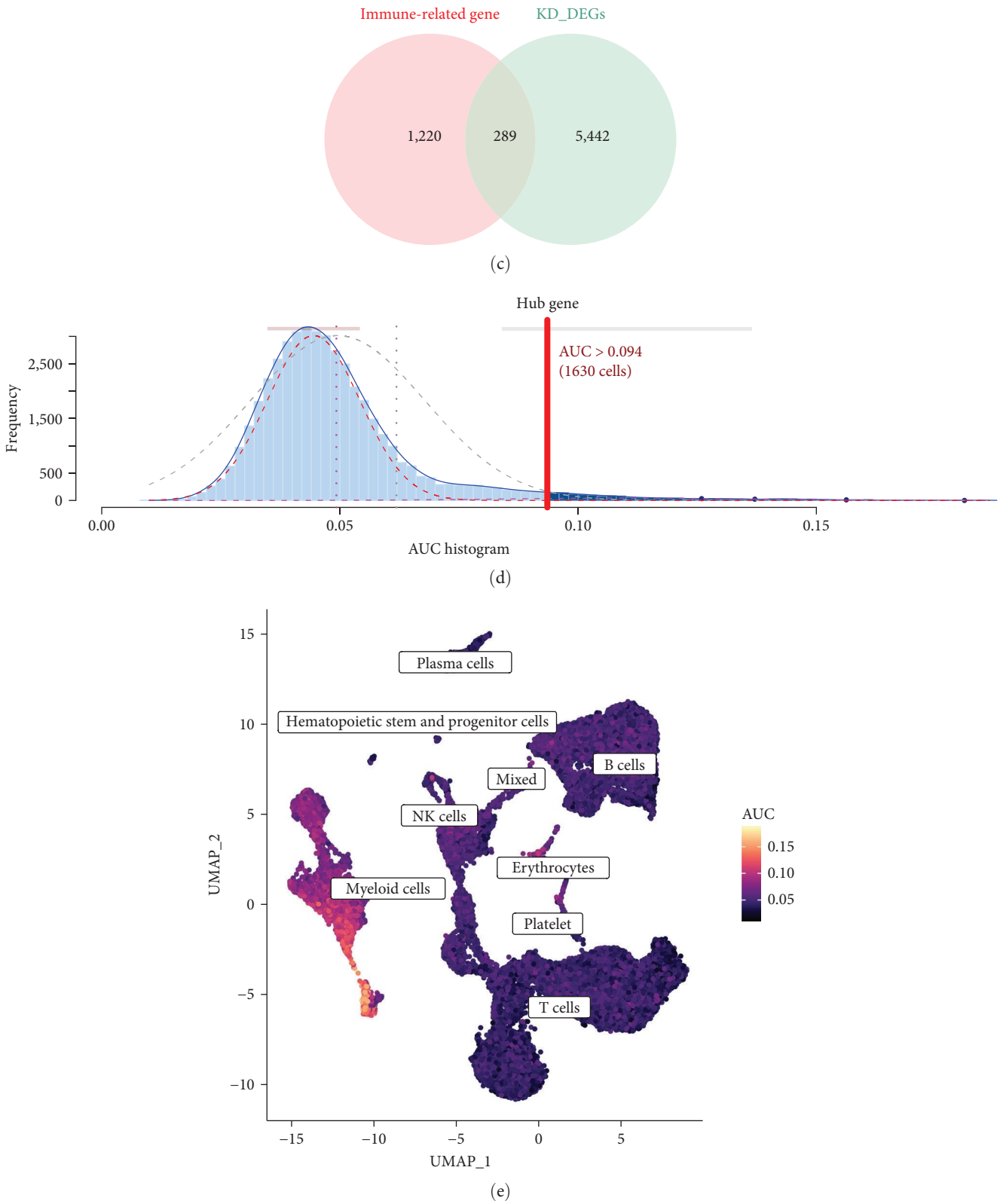

FIGURE 5: DEGs of KD from the GSE18606 dataset. (a) Volcano plot of DEGs ($|\log FC| \geq 0.25$ and adjusted $P < 0.05$). Upregulated genes are in red and downregulated genes are in blue. The first 20 DEGs are tagged. (b) GO of DEGs in GSE18606, showing enrichment in G protein-coupled receptor binding, neutrophil chemotaxis, intercellular adhesion, and inflammatory cytokine production. (c) Venn diagram showing 289 IRGs from the DEGs in KD. (d) Scores of 289 screened IRGs. (e) UMAP plots of IRG scores in all clusters. Myeloid cells express more genes and exhibit higher AUC values.

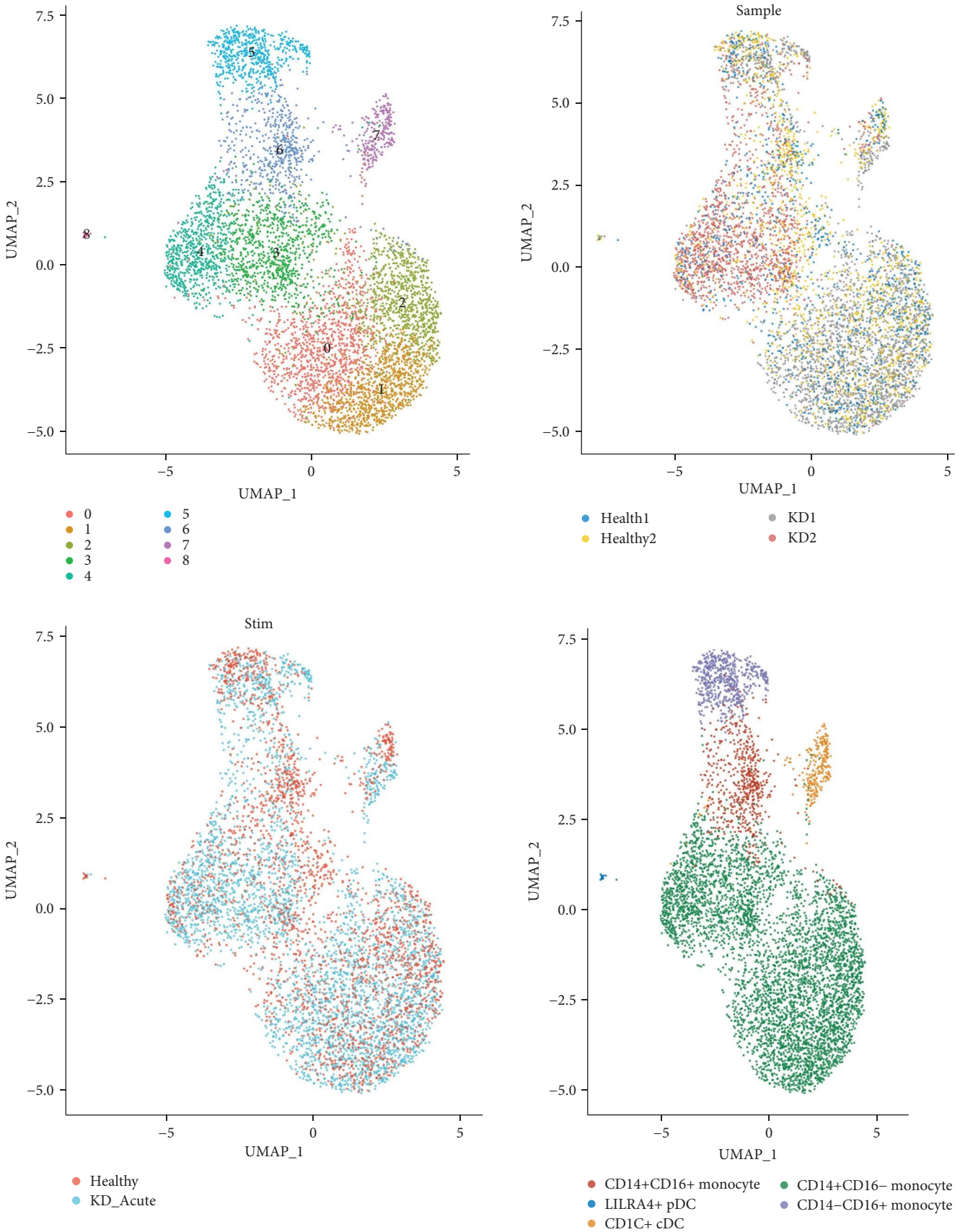

(a)

Figure 6: Continued.

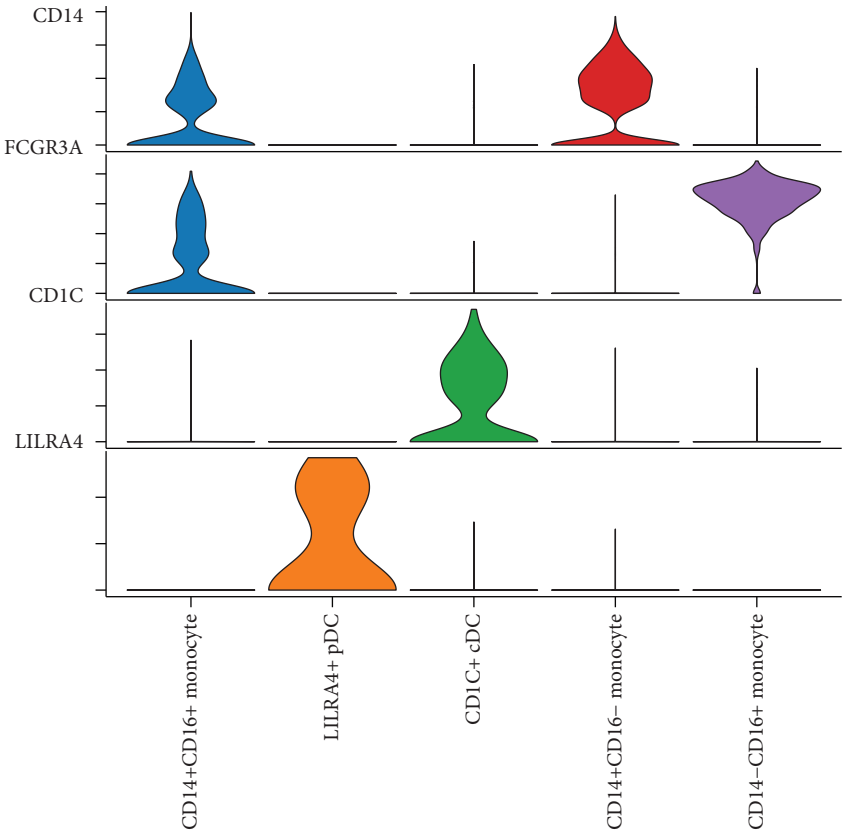

(b)

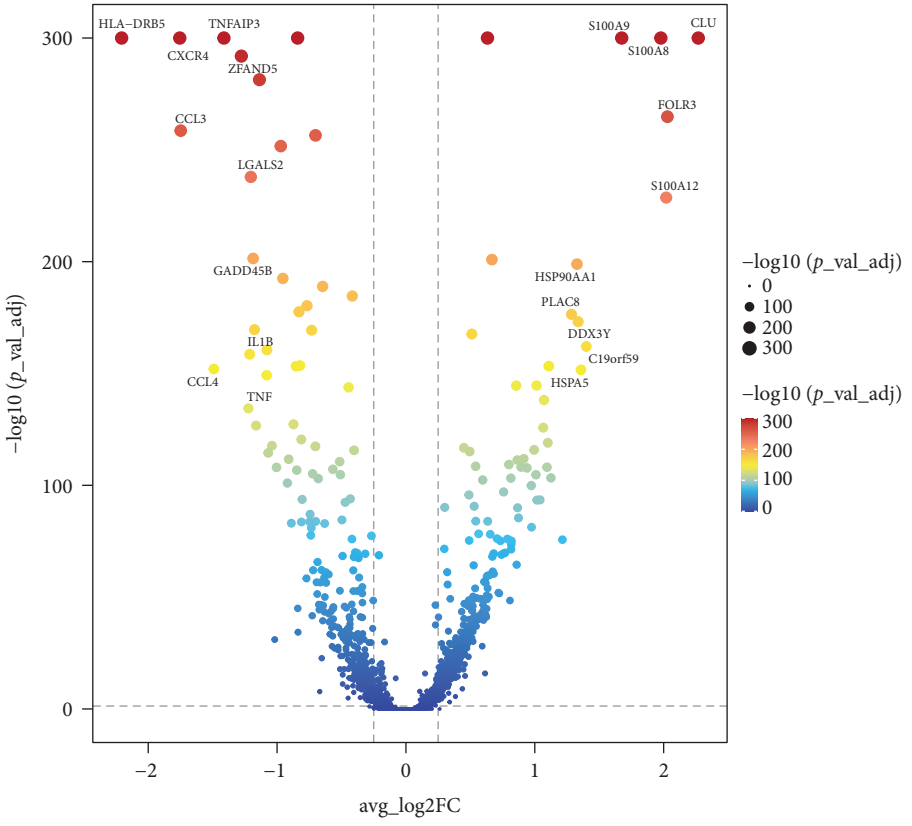

(c)

Figure 6: Continued.

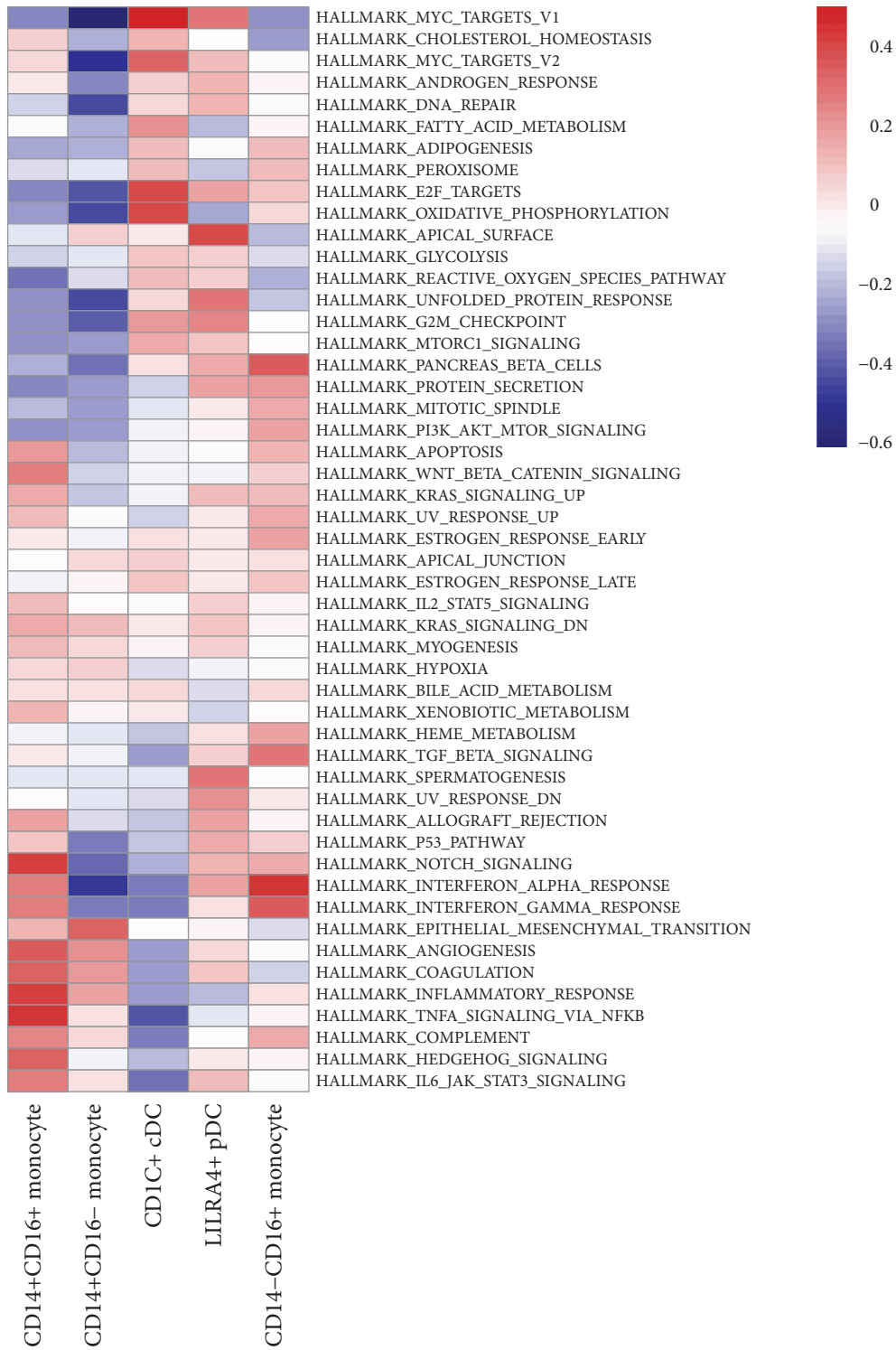

(d)

Figure 6: Cluster analysis of myeloid cells in KD from the GSE15245 dataset. (a) Cell types identified in myeloid cells using UMAP. (b) Violin plot depicts distributions of cell-type marker genes in monocytes and LILRA4 + pCD. (c) Volcano plot of DEGs in monocytes from KD patients. Upregulated genes are in red and downregulated genes are in blue. (d) Gene set variation analysis (GSVA) of significant hallmarks in monocytes, showing that DEGs are mainly involved in the regulation of immune response and TNFA signaling via NFKB.

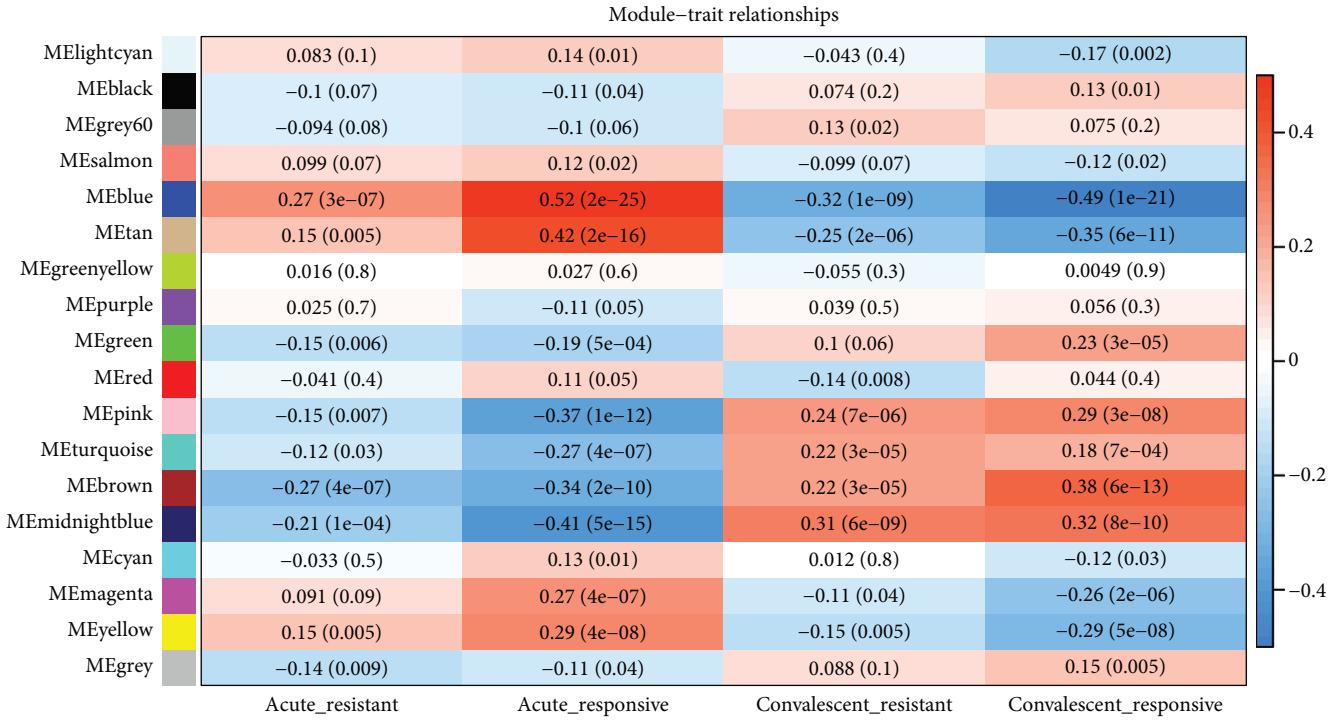

(a)

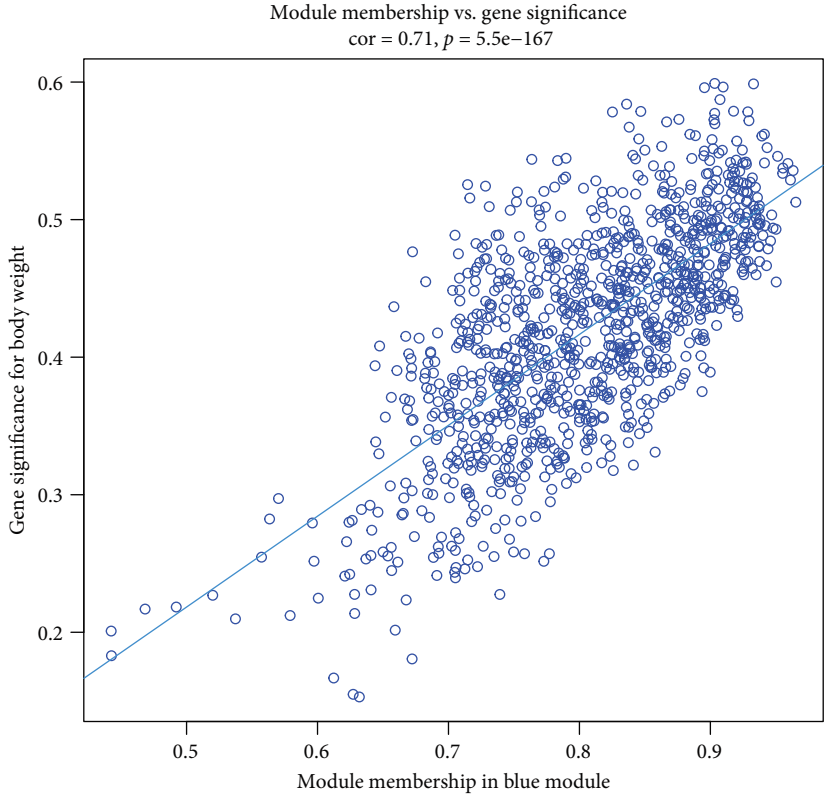

(b)

Figure 7: Continued.

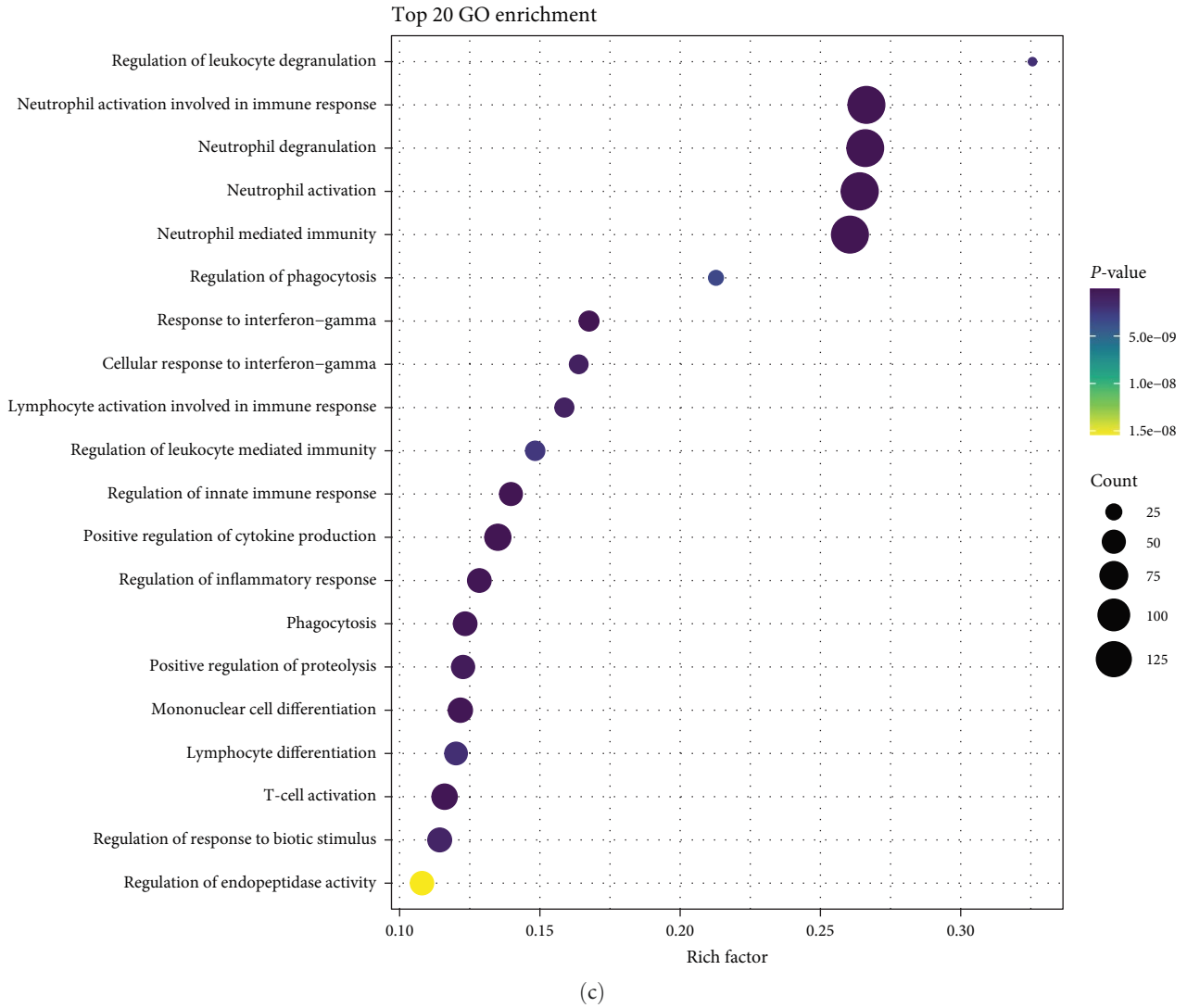

(c)

Figure 7: Analysis of DEGs across KD phenotypes (GSE63881): acute IVIG-responsive KD, acute IVIG-resistant KD, convalescent IVIG-responsive KD, and convalescent IVIG-resistant KD. (a) Cluster analysis of differentially expressed IRGs. Each color represents a module in the gene coexpression network constructed using weighted gene coexpression network analysis (WGCNA). (b) Membership in the blue module, showing DEGs that were positively correlated with IVIG-responsive KD phenotypes. (c) These DEGs are primarily associated with neutrophil activation, neutrophil degranulation, and neutrophil-mediated immunity.

genes were mainly enriched in innate immune pathways, such as neutrophil activation, neutrophil degranulation, and neutrophil-mediated immunity (Figure 7(c)).

In addition, analysis of GSE18606 revealed 3,598 DEGs (1,570 upregulated and 2,028 downregulated) between acute IVIG-responsive and acute IVIG-resistant KD (Figure 8(a), Table S4). These DEGs were mainly enriched in neutrophil activation, degranulation, and neutrophil-mediated immunity (Figure 8(b)). Intersection analysis yielded 48 IRGs from the DEGs (Figure 8(c)) that were mostly involved in regulation of the innate immune response (Figure 8(d)). In addition, they were expressed in myeloid cells and $CD14^{+}CD16^{+}$ monocytes (Figures 9(a) and 9(b)). The PPI network analysis indicated that inflammation-related genes *IL1R1*, *SOCS3*, *IL1R2*, *TLR8*, *IL1RN*, *CCR1*, *IL1B*, *IL4R*, *IL10RB*, and *IFNGR1* were hub genes (Figure 9(c)).

3.7. RT-qPCR Validation of Hub Genes in Chinese KD Patients. To further validate the expression of the ten hub genes in KD patients, we detected their expression in 18 samples of peripheral venous blood from KD patients (10 IVIG responsive, 8 IVIG nonresponsive) and 10 samples from healthy controls. The results showed that the expression of *IL1R1* ($P<0.01$), *SOCS3* ($P<0.01$), *TLR8* ($P<0.01$), *CCR1* ($P<0.01$), *IL1B* ($P<0.01$), and *IL10RB* ($P<0.001$) was significantly up-regulated in the IVIG nonresponsive KD group compared with the control group and the IVIG responsive KD group. The expression of *IL1R2* ($P<0.01$), *IL1RN* ($P<0.01$), *IL4R* ($P<0.01$), and *IFNGR1* ($P<0.01$) was significantly up-regulated in the IVIG nonresponsive KD group compared to the control group, but there was no significant difference compared to the IVIG responsive group (Figure 10).

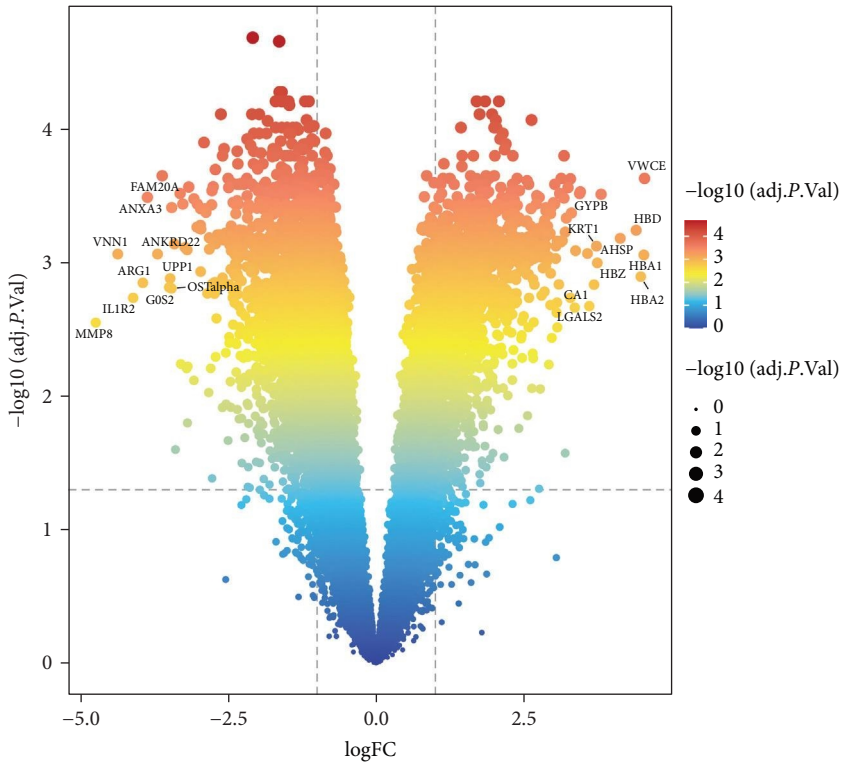

(a)

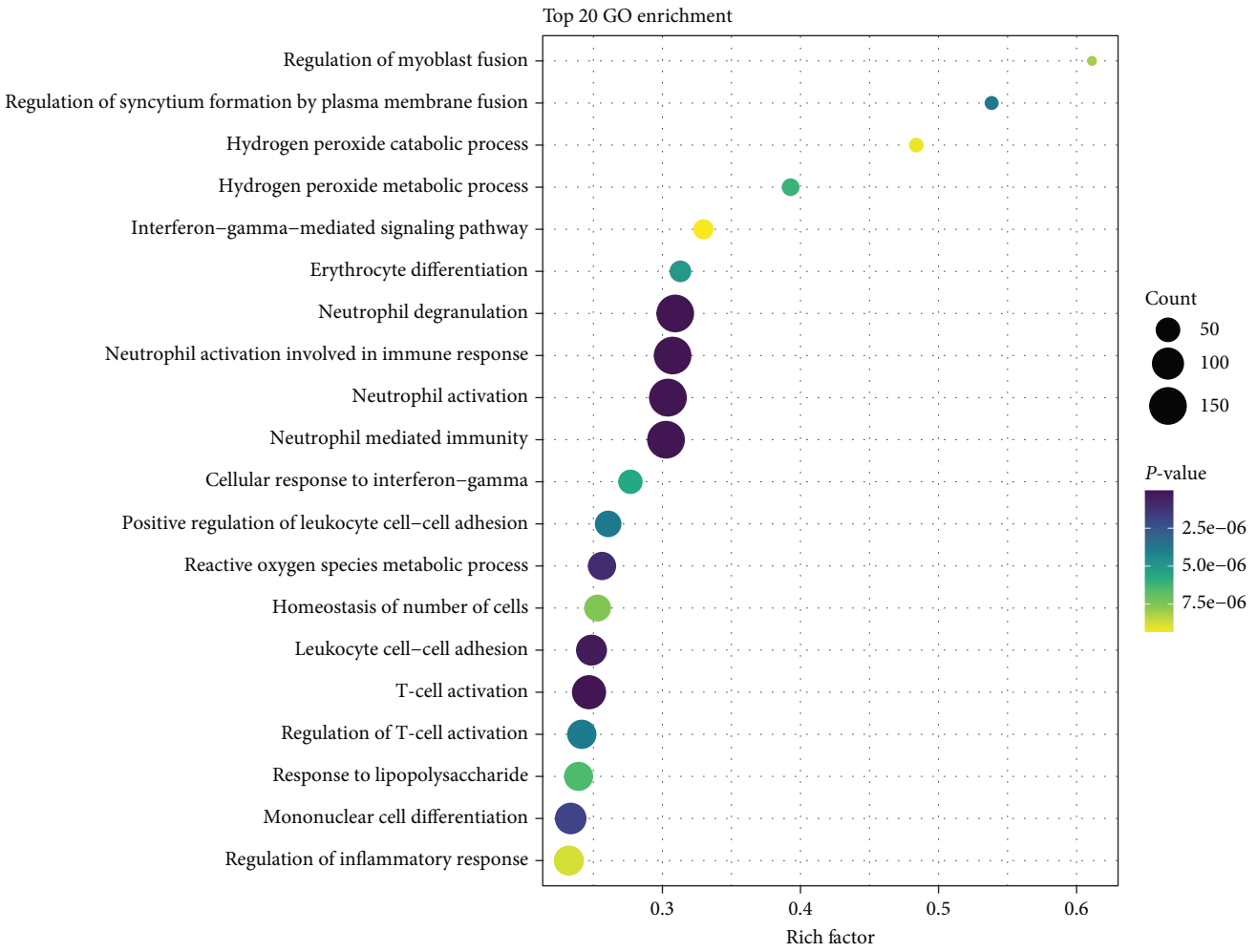

(b)

Figure 8: Continued.

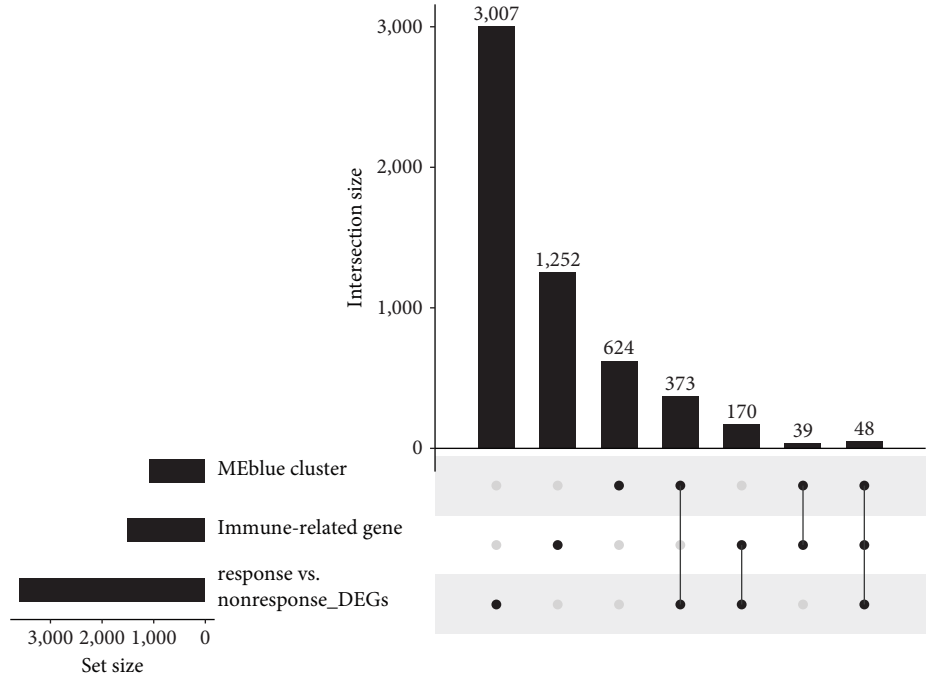

(c)

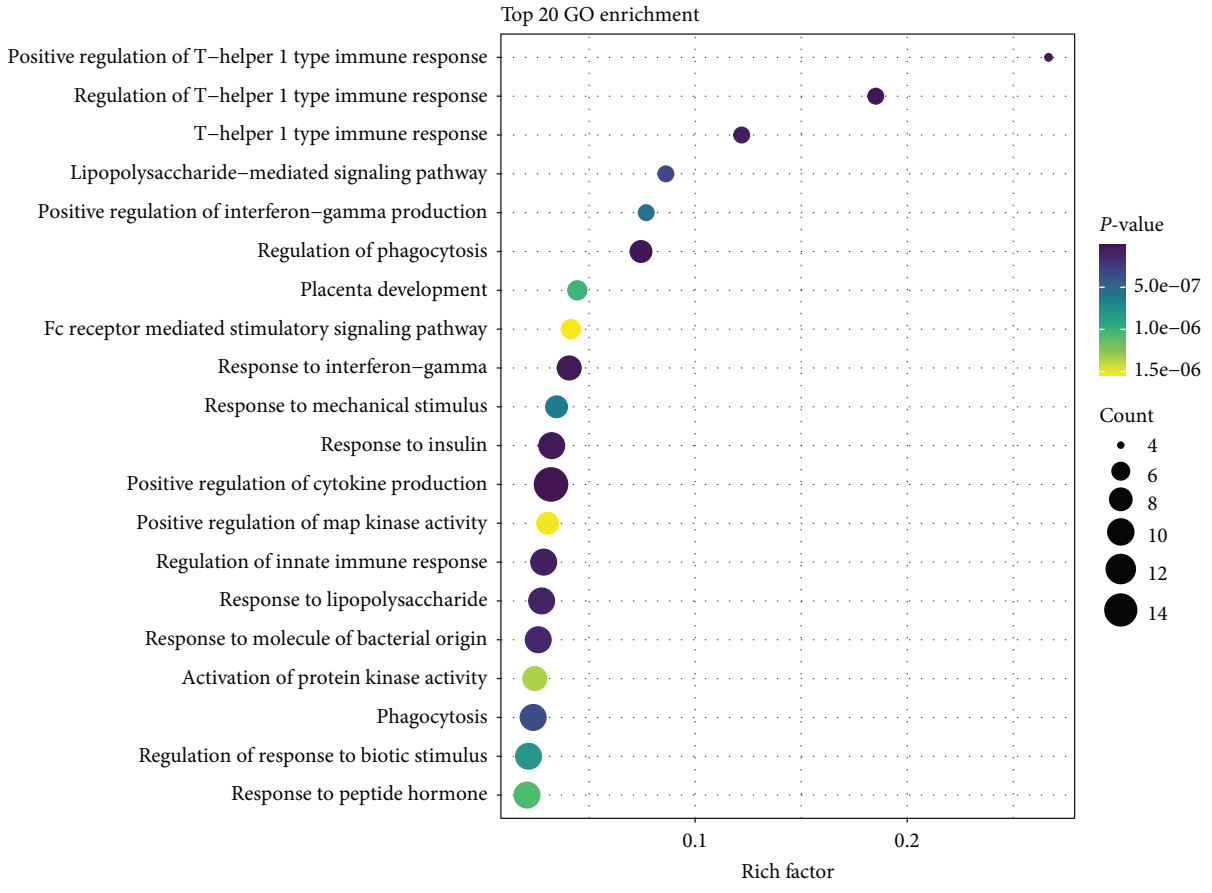

(d)

Figure 8: Analysis of DEGs between acute IVIG-responsive KD and acute IVIG-resistant KD (GSE18606). (a) Volcano plot of DEGs ($|\log FC| \geq 1$ and adjusted $P < 0.05$). The adjusted P-value levels are indicated by the color of the dot, with the top 20 differentially expressed genes (DEGs) being specifically labeled. Upregulated genes are on the right and downregulated genes on the left. (b) These DEGs are mainly involved in neutrophil activation, neutrophil degranulation, and neutrophil-mediated immunity. (c) Intersection analysis of IVIG-related DEGs between the two datasets (GSE63881 and GSE18606). (d) The DEGs found in both datasets are associated with positive regulation of T-helper 1 type immune response and lipopolysaccharide-mediated signaling pathway.

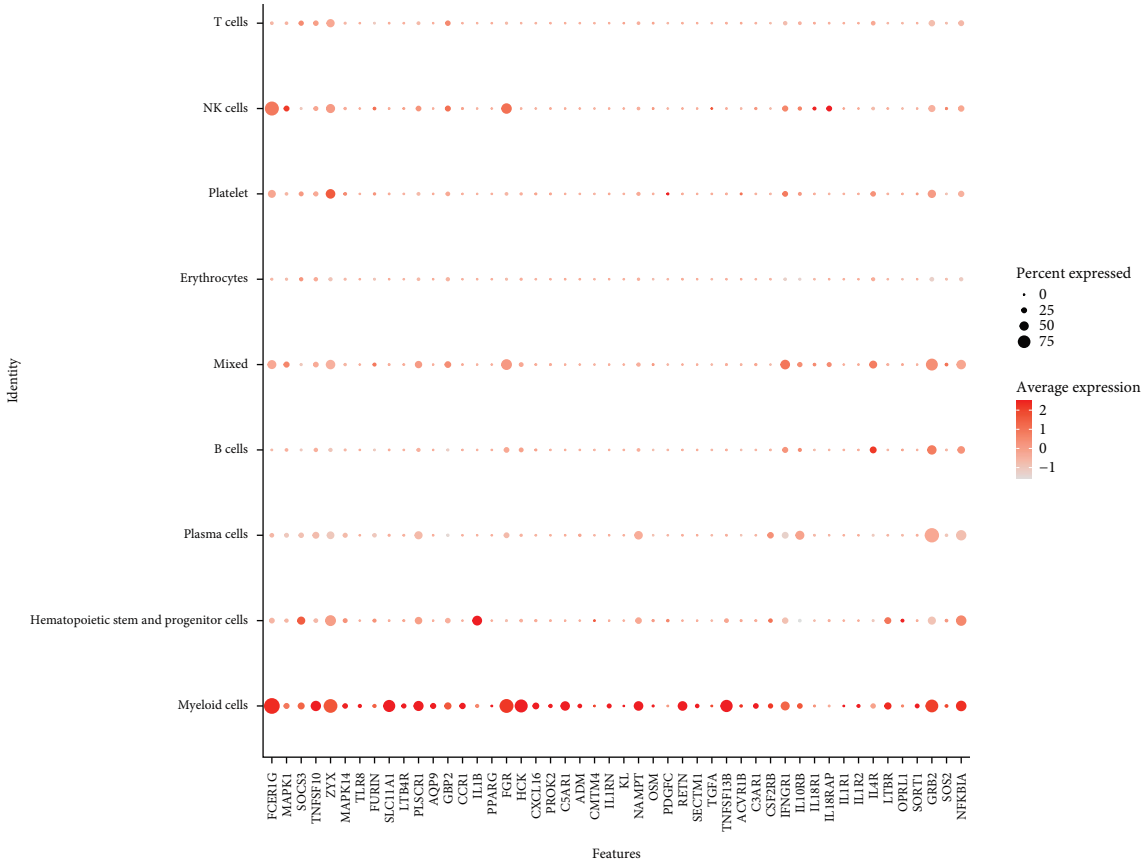

(a)

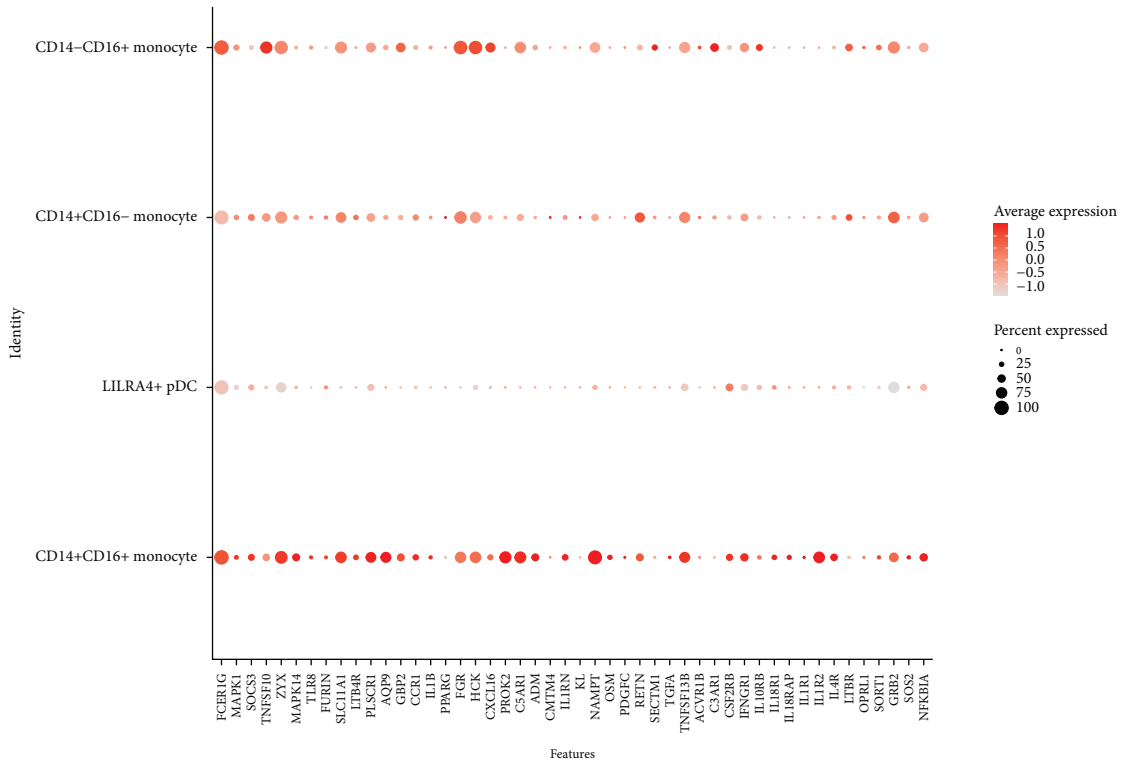

(b)

Figure 9: Continued.

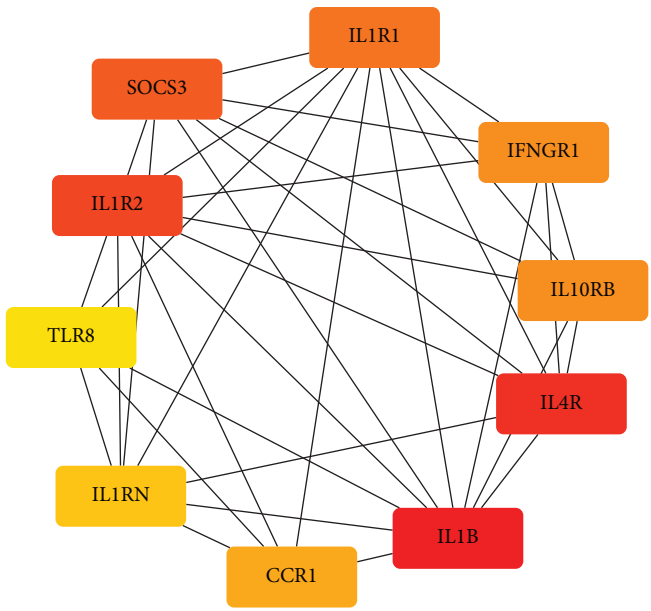

(c)

Figure 9: Distribution of DEGs in immune cells. (a) The DEGs are mainly found in myeloid cells, specifically (b) $CD14^{+}CD16^{+}$ monocytes and $CD14^{-}CD16^{+}$ monocytes. (c) The PPI network analysis of common hub genes.

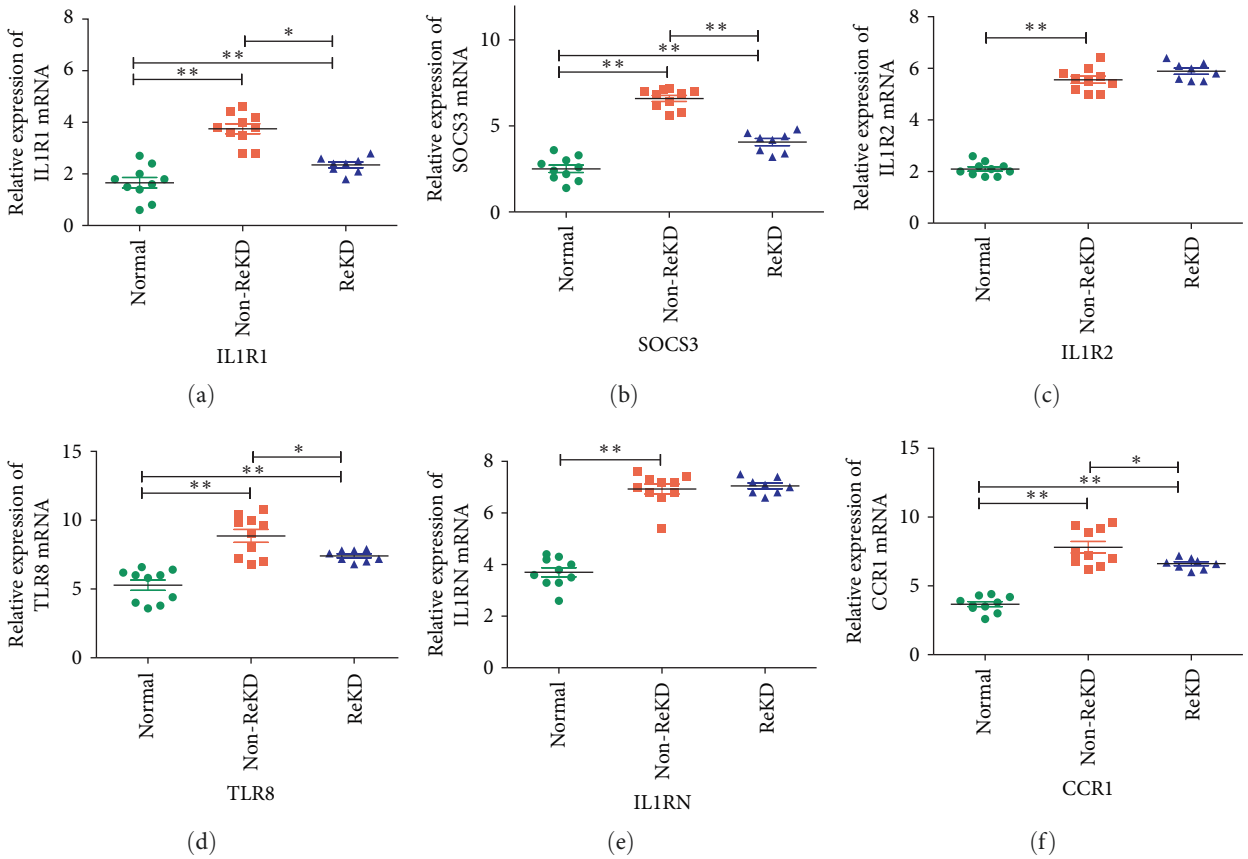

Figure 10: Continued.

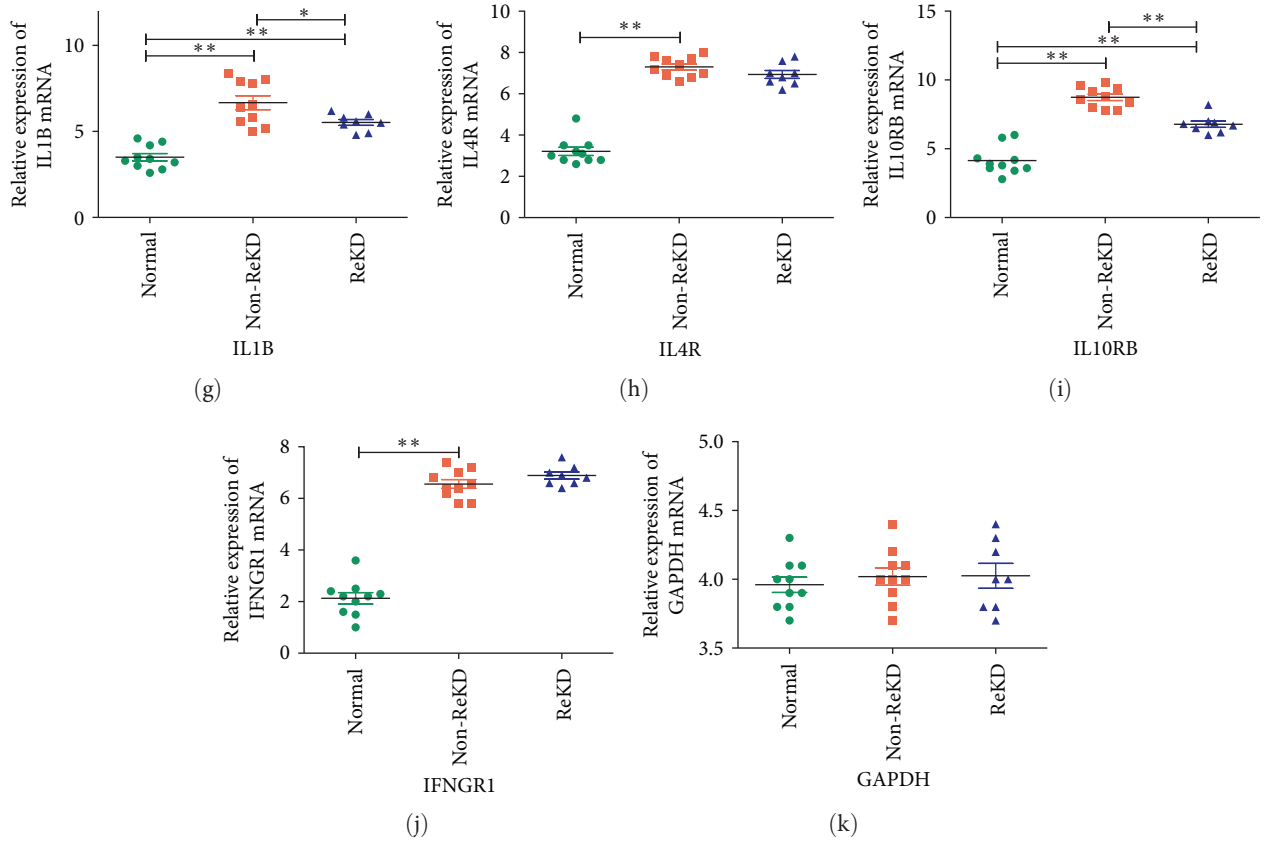

Figure 10: RT-qPCR validation of hub genes in KD patients. (a) Expression level of IL1R1 gene, (b) expression level of SOCS3 gene, (c) expression level of IL1R2 gene, (d) expression level of TLR8 gene, (e) expression level of IL1RN gene, (f) expression level of CCR1 gene, (g) expression level of IL1B gene, (h) expression level of IL4R gene, (i) expression level of IL10RB gene, (j) expression level of IFNGR1 gene, and (k) expression level of GAPDH gene. ReKD = IVIG responsive KD ($n = 10$), Non-ReKD = IVIG nonresponsive KD ($n = 8$). $^{*}P < 0.05$, $^{**}P < 0.01$.

Table 4: Comparison of the IVIG-responsive and -resistant patients with KD in terms of demographic and clinical variables.

Variable	IVIG-responsive ($n = 133$)	IVIG-resistant ($n = 18$)	P-value
Age (months)	21.9 (13.2, 40.5)	27.95 (16.2, 35.5)	0.918
Male (n, percentage)	86 (64.7%)	13 (72.2%)	0.528
CRP (mg/L)	80 (45.9, 111.0)	121.5 (82.9, 148.2)	0.026
PCT (ng/mL)	0.5 (0.2, 1.2)	1.2 (0.3, 3.1)	0.09
WBC ($\times 10^9$/L)	14.3 (11.5, 19.0)	15.2 (11.8, 26.1)	0.789
NEUT ($\times 10^9$/L)	8.9 (6.5, 11.9)	10.7 (8.3, 16.2)	0.325
LYM ($\times 10^9$/L)	3.7 (2.6, 6.0)	2.9 (0.9, 6.5)	0.03
MONO ($\times 10^9$/L)	0.9 (0.6, 1.3)	1.0 (0.5, 1.5)	0.945
PLT ($\times 10^9$/L)	383 (310.5, 493.5)	372.5 (229.7, 459.7)	0.308
NLR	2.5 (1.5, 3.5)	3.7 (1.5, 13.1)	0.012

Note. CRP, C-reactive protein; PCT, procalcitonin; WBC, white blood cells; NEUT, neutrophil; LYM, lymphocyte; MONO, monocytes; PLT, platelet; NLR, neutrophil/lymphocyte ratio. The data are presented as Median (interquartile spacing) or number (%).

3.8. Inflammatory Markers in KD Patients. We investigated 151 KD patients, including 133 IVIG-responsive individuals and 18 IVIG-resistant individuals (Table 4). The two patient groups did not differ in age or sex. The IVIG-resistant group had higher CRP, PCT, and NLR levels than the IVIG-responsive group. Additionally, the IVIG-resistant group had significantly lower lymphocyte levels than the IVIG-responsive group.

4. Discussion

Increasing evidence suggests that the innate immune response may be involved in KD pathogenesis [13, 14, 36]. Of particular note is the involvement of monocytes, innate immune cells from the bone marrow that have multiple functions, including tissue development and homeostasis, inflammation initiation and resolution, and tissue repair [37–39]. Monocytes are involved in the pathogenesis of other cardiovascular diseases [40–42], and changes in monocyte subsets have been observed in KD patients [16]. Other evidence to suggest that innate immunity plays a major role in KD pathogenesis includes research using mouse models of the disease. One such study identified a nucleotide-binding oligomerization domain-containing protein (NOD) 1 ligand as an important inducer of coronary arteritis [43]. Another study using a mouse model found that inhibition of interleukin-1β attenuates vasculitis [44].

Here, we followed up on those previous reports in an effort to better understand the potential mechanisms of innate immunity in KD pathogenesis. Through an analysis of scRNA sequencing data and marker gene expression, we first found that T cells in patients with KD were significantly reduced (Figure 1(d)), and also confirmed that myeloid cells —the main source of monocytes—were the most heterogeneous cell group (Figure 2(a)). Our results corroborated earlier research showing changes to T cells in KD patients [13, 14], but myeloid cells have rarely been studied in KD, although their involvement has been confirmed in various other inflammatory diseases [42, 45]. Here, functional analyses revealed that DEGs in myeloid cells were closely related to inflammatory response and cytokine regulation (Figures 2(d) and 2(e)), implicating them in the development of KD. Our subgroup analysis then revealed that myeloid cells in KD patients were mainly composed of monocytes and LILR4$^+$pDC. Monocytes can be broken down into three subtypes: CD14$^+$CD16$^+$, CD14$^+$CD16$^-$, and CD14$^-$CD16$^+$ [46], or intermediate, classical, and nonclassical in humans. Our observed monocyte composition was consistent with previous studies [16]. We also noted that the DEGs *S100A12*, *S100A9*, *S100A8*, and *ITGAM* were primarily expressed in CD14$^+$CD16$^+$ monocytes (Figure 3(c)). Previous studies have found that patients with acute KD had higher circulating concentrations of S100A8/9 heterodimer and S100A12 than patients with fever caused by other diseases; IVIG treatment decreased these concentrations [47, 48]. Even after the acute stage, KD patients with large coronary aneurysms maintained higher S100A8/9 heterodimer levels [47]. In addition, elevated *S100A8*, *S100A9*, and *S100A12* levels have been found in inflammatory diseases associated with immune disorders, such as juvenile idiopathic arthritis [49]. Hence, the increased levels of S100A8, S100A9, and S100A12 proteins cannot be exclusively attributed to KD. In addition, integrin *ITGAM* was upregulated in KD vasculopathy [50]. Furthermore, we observed elevated expression of inflammatory regulation genes associated with CD14$^+$CD16$^+$ cells (Figure 3(c)), and GSVA indicated that this monocyte subtype is important to the inflammatory response in KD (Figure 4(b)). Similarly, recent reports have shown that, in addition to having high antigen presentation capacity, CD14$^+$CD16$^+$ cells highly express proinflammatory cytokines [51, 52]. Data from peripheral blood of KD patients also revealed a link between these cells and inflammation [53]. Taken together, our study and previous research all indicate that CD14$^+$CD16$^+$ monocytes are heavily involved in the inflammatory response of acute KD.

Changes in the trajectory of monocyte development are closely related to disease occurrence [54, 55]. Here, pseudotime analysis of monocyte subsets revealed a trajectory from CD14$^-$CD16$^+$ monocytes to CD14$^+$CD16$^+$ monocytes (Figure 3(d)), contradicting earlier research showing that CD14$^+$CD16$^-$ monocytes are significantly elevated in acute KD [16]. Moreover, during monocyte development, inflammation-related gene expression increased, but their expression in CD14$^+$CD16$^+$ monocytes actually decreased at the end of the developmental trajectory. By contrast, the expression of inflammatory transcription factors was significantly higher in CD14$^+$CD16$^+$ monocytes (Figure 4(b)). Therefore, we speculate that CD14$^+$CD16$^+$ monocytes are the final effector cells in acute KD and that they regulate cytokine levels by promoting the expression of inflammatory transcription factors.

Although IVIG is an effective treatment for KD, drug resistance rates are high [56, 57]. Because IVIG-resistance is associated with an increased incidence of coronary artery aneurysms, IVIG-resistant patients should be identified before initiating treatment because they may benefit from additional anti-inflammatory therapy. In this study, we therefore analyzed multiple GEO scRNA datasets to identify potential genetic markers that could distinguish between IVIG-resistant and -responsive patients. Our results revealed that IVIG-responsive patients had highly synergistic differential genes (Figures 7(a) and 7(b)) that are involved in neutrophil activation and degranulation (Figures 7(c) and 8). Neutrophils are a critical part of innate immunity but can have harmful effects if excessively activated [58], causing immune diseases such as rheumatoid arthritis [59, 60] and vasculitis [61, 62]. Elevated peripheral neutrophils in patients with KD are associated with coronary artery dilation and IVIG resistance [63, 64]. The NLR is a comprehensive indicator of neutrophil activation and immune disorders that also plays an important role in KD [64, 65]. Here, our clinical data revealed that IVIG-resistant patients had higher NLR than IVIG-responsive patients, validating the results of scRNA sequencing.

Further analysis showed that DEGs associated with neutrophils were mainly expressed in CD14$^+$CD16$^+$ and CD14$^-$CD16$^+$ monocytes (Figures 9(a) and 9(b)). In addition, the effect of IVIG on acute KD is closely related to the expression of immunomodulatory genes that activate neutrophils in these two monocyte subsets. The PPI network analysis then revealed that all hub genes in KD (Figure 9(c)) are inflammation-related genes that regulate the innate immune system. Broadly, these results corroborate a prior genome-wide transcriptome analysis demonstrating that increased CD177 transcript levels activate neutrophils and

are closely related to KD [66]. Autopsy results of patients who died during the acute phase of KD suggest neutrophilic involvement in damage to the coronary arteries [67]. Consistent with our results, it has been found that the hub gene *CCR1* is an important gene in the pathogenesis of KD [15]. The hub genes *TLR8* and *IL1B* are also closely related to neutrophil degranulation in patients with KD [68]. All available data thus provide evidence of neutrophil activation being crucial to KD pathogenesis. Furthermore, it has been observed that *IL1B*, *SOCS3*, and *IL1RN* exhibit high expression levels in other autoimmune diseases that are closely linked to impaired innate immune function [69].

Although there are many clinical predictors of IVIG nonresponse in KD, the clinical application value is limited. In our study, we screened for hub genes by analyzing the expression of differential genes in monocytes of KD patients with IVIG response and IVIG nonresponse, and these results were further verified using RT-qPCR. The validated results indicated that the expression of *IL1R1* ($P<0.01$), *SOCS3* ($P<0.01$), *TLR8* ($P<0.01$), *CCR1* ($P<0.01$), *IL1B* ($P<0.01$), and *IL10RB* ($P<0.001$) was significantly up-regulated in the IVIG nonresponsive group compared with that in the control group and the IVIG responsive group, while *IL1R2* ($P<0.01$), *IL1RN* ($P<0.01$), *IL4R* ($P<0.01$), and *IFNGR1* ($P<0.01$) were significantly up-regulated in the IVIG nonresponsive group compared to that in the normal group, but there was no significant difference compared to the IVIG responsive group (Figure 10). The results suggested that *IL1R1*, *SOCS3*, *TLR8*, *CCR1*, *IL1B*, and *IL10RB* could be used as hub genes for screening IVIG responsive and IVIG nonresponsive patients of KD.

To our knowledge, this is the first study to elaborate on the role of innate immunity in the pathogenesis of KD and the mechanism of IVIG resistance. Combining both scRNA-seq and microarray data analysis, our data strongly illustrates the involvement of innate immunity in the pathogenesis of KD and provides insights into the mechanism of IVIG resistance. Specifically, abnormal expression of immunomodulatory genes in $CD14^{+}CD16^{+}$ and $CD14^{-}CD16^{+}$ monocytes seems to trigger neutrophil activation, causing the worst symptoms of the disease and influencing the response to IVIG. The limitations of this study are as follows: first, as the study mainly relied on published RNA microarray datasets and RNA sequencing datasets for analysis, key clinical data could not be obtained. Second, the mechanism of action of these identified hub genes needs to be further studied.

Data Availability

The datasets presented in this study can be found in online repositories. The names of the repository/repositories and accession number(s) can be found in the article/Supplementary Material.

Ethical Approval

This study was carried out in accordance with the guidelines of the Ethics Committee of the First Affiliated Hospital of Sun Yat-sen University. The protocol was approved by the Ethics Committee of the First Affiliated Hospital of Sun Yat-sen University ((2022) 514).

Conflicts of Interest

The authors declare that the research was conducted in the absence of any commercial or financial relationships that could be construed as a potential conflicts of interest.

Authors' Contributions

Hongjun Ba, Yao Wang, and Lili Zhang contributed in the conceived and designed the study. Jixun Lin and Youzhen Qin contributed in the collected data. Hongjun Ba contributed in the wrote the paper. All authors contributed to the article and approved the submitted version. Hongjun Ba and Lili Zhang contributed equally to this work and shared first authorship.

Acknowledgments

The study was supported by the Guangdong Basic and Applied Basic Research Foundation (2020A1515010184). We thank Dr. Jianming Zeng (University of Macau), and all the members of his bioinformatics team, biotrainee, for generously sharing their experience and codes. We also thank for generous help from Dr. Xiufeng Liu.

Supplementary Materials

Supplementary Material: dissolution Cure of RT-qPCR Experimental Genes. Figure S1: genes (features), counts, and mitochondrial gene percentage of each samples. Figure S2: marker genes in each cluster. Figure S3: marker genes in myeloid cells. Table S1: all marker-celltype-deg.csv. Table S2: 381-IRG.csv. Table S3: GSE18606_DEG_IRG_289. Table S4: GSE18606-deg-Respond_nonrespond_Acute.csv. (*Supplementary Materials*)

References

[1] T. Kawasaki, "Acute febrile mucocutaneous syndrome with lymphoid involvement with specific desquamation of the fingers and toes in children," *Arerugi*, vol. 16, no. 3, pp. 178–222, 1967.

[2] H. Ba, Y. Wang, L. Zhang, H. Wang, Z.-P. Huang, and Y. Qin, "Prediction of immune infiltration diagnostic gene biomarkers in Kawasaki disease," *Journal of Immunological Research*, vol. 2022, Article ID 8739498, 16 pages, 2022.

[3] K. Takahashi, T. Oharaseki, Y. Yokouchi, N. Hiruta, and S. Naoe, "Kawasaki disease as a systemic vasculitis in childhood," *Annals of Vascular Diseases*, vol. 3, no. 3, pp. 173–181, 2010.

[4] K. Takahashi, T. Oharaseki, and Y. Yokouchi, "Histopathological aspects of cardiovascular lesions in Kawasaki disease," *International Journal of Rheumatic Diseases*, vol. 21, no. 1, pp. 31–35, 2018.

[5] J. Kim, C. Shimizu, M. He et al., "Endothelial cell response in Kawasaki disease and multisystem inflammatory syndrome in children," *International Journal of Molecular Sciences*, vol. 24, no. 15, Article ID 12318, 2023.

[6] S. T. Shulman and A. H. Rowley, "Kawasaki disease: insights into pathogenesis and approaches to treatment," *Nature Reviews Rheumatology*, vol. 11, no. 8, pp. 475–482, 2015.

[7] T. J. Brown, S. E. Crawford, M. L. Cornwall, F. Garcia, S. T. Shulman, and A. H. Rowley, "CD8 T lymphocytes and macrophages infiltrate coronary artery aneurysms in acute Kawasaki disease," *The Journal of Infectious Diseases*, vol. 184, no. 7, pp. 940–943, 2001.

[8] A. H. Rowley, C. A. Eckerley, H. M. Jäck, S. T. Shulman, and S. C. Baker, "IgA plasma cells in vascular tissue of patients with Kawasaki syndrome," *The Journal of Immunology*, vol. 159, no. 12, pp. 5946–5955, 1997.

[9] A. H. Rowley, S. T. Shulman, C. A. Mask et al., "IgA plasma cell infiltration of proximal respiratory tract, pancreas, kidney, and coronary artery in acute Kawasaki disease," *The Journal of Infectious Diseases*, vol. 182, no. 4, pp. 1183–1191, 2000.

[10] D. Y. Leung, R. S. Geha, J. W. Newburger et al., "Two monokines, interleukin 1 and tumor necrosis factor, render cultured vascular endothelial cells susceptible to lysis by antibodies circulating during Kawasaki syndrome," *Journal of Experimental Medicine*, vol. 164, no. 6, pp. 1958–1972, 1986.

[11] D. Y. M. Leung, E. Kurt-Jones, J. W. Newburger, R. S. Cotran, J. C. Burns, and J. S. Pober, "Endothelial cell activation and high interleukin-1 secretion in the pathogenesis of acute Kawasaki disease," *The Lancet*, vol. 334, no. 8675, pp. 1298–1302, 1989.

[12] J.-M. Zhao and X.-H. Wang, "Clinical significance of anti-neutrophil cytoplasmic antibodies and anti-endothelial cell antibodies in children with Kawasaki disease," *Chinese Journal of Contemporary Pediatrics*, vol. 16, no. 7, pp. 740–744, 2014.

[13] X. Fan, Y. Zhou, X. Guo, and M. Xu, "Utilizing single-cell RNA sequencing for analyzing the characteristics of PBMC in patients with Kawasaki disease," *BMC Pediatrics*, vol. 21, no. 1, Article ID 277, 2021.

[14] Z. Wang, L. Xie, G. Ding et al., "Single-cell RNA sequencing of peripheral blood mononuclear cells from acute Kawasaki disease patients," *Nature Communications*, vol. 12, no. 1, Article ID 5444, 2021.

[15] H. Nie, S. Wang, Q. Wu, D. Xue, and W. Zhou, "Five immune-gene-signatures participate in the development and pathogenesis of Kawasaki disease," *Immunity, Inflammation and Disease*, vol. 9, no. 1, pp. 157–166, 2021.

[16] Z. Geng, Y. Tao, F. Zheng et al., "Altered monocyte subsets in Kawasaki disease revealed by single-cell RNA-sequencing," *Journal of Inflammation Research*, vol. 14, pp. 885–896, 2021.

[17] M. Dhaliwal, R. Tyagi, P. Malhotra et al., "Mechanisms of immune dysregulation in COVID-19 are different from SARS and MERS: a perspective in context of Kawasaki disease and MIS-C," *Frontiers in Pediatrics*, vol. 10, Article ID 790273, 2022.

[18] B. S. Moffett, D. Syblik, S. Denfield, C. Altman, and K. Tejtel-Sexson, "Epidemiology of immunoglobulin resistant Kawasaki disease: results from a large, national database," *Pediatric Cardiology*, vol. 36, no. 2, pp. 374–378, 2015.

[19] Y. Lu, K. Li, Y. Hu, and X. Wang, "Expression of immune related genes and possible regulatory mechanisms in Alzheimer's disease," *Frontiers in Immunology*, vol. 12, Article ID 768966, 2021.

[20] F. Chen, J. Song, Z. Ye et al., "Integrated analysis of cell cycle-related and immunity-related biomarker signatures to improve the prognosis prediction of lung adenocarcinoma," *Frontiers in Oncology*, vol. 11, Article ID 666826, 2021.

[21] W. Fury, A. H. Tremoulet, V. E. Watson et al., "Transcript abundance patterns in Kawasaki disease patients with intravenous immunoglobulin resistance," *Human Immunology*, vol. 71, no. 9, pp. 865–873, 2010.

[22] L. T. Hoang, C. Shimizu, L. Ling et al., "Global gene expression profiling identifies new therapeutic targets in acute Kawasaki disease," *Genome Medicine*, vol. 6, no. 11, Article ID 541, 2014.

[23] T. Stuart, A. Butler, P. Hoffman et al., "Comprehensive integration of single-cell data," *Cell*, vol. 177, no. 7, pp. 1888–1902.E21, 2019.

[24] X. Qiu, A. Hill, J. Packer, D. Lin, Y.-A. Ma, and C. Trapnell, "Single-cell mRNA quantification and differential analysis with Census," *Nature Methods*, vol. 14, no. 3, pp. 309–315, 2017.

[25] L. Garcia-Alonso, C. H. Holland, M. M. Ibrahim, D. Turei, and J. Saez-Rodriguez, "Benchmark and integration of resources for the estimation of human transcription factor activities," *Genome Research*, vol. 29, no. 8, pp. 1363–1375, 2019.

[26] S. Bhattacharya, P. Dunn, C. G. Thomas et al., "ImmPort, toward repurposing of open access immunological assay data for translational and clinical research," *Scientific Data*, vol. 5, no. 1, Article ID 180015, 2018.

[27] D. Zeng, Z. Ye, R. Shen et al., "IOBR: multi-omics immuno-oncology biological research to decode tumor microenvironment and signatures," *Frontiers in Immunology*, vol. 12, Article ID 687975, 2021.

[28] M. E. Ritchie, B. Phipson, D. Wu et al., "Limma powers differential expression analyses for RNA-sequencing and microarray studies," *Nucleic Acids Research*, vol. 43, no. 7, Article ID e47, 2015.

[29] P. Langfelder and S. Horvath, "WGCNA: an R package for weighted correlation network analysis," *BMC Bioinformatics*, vol. 9, no. 1, Article ID 559, 2008.

[30] T. Wu, E. Hu, S. Xu et al., "ClusterProfiler 4.0: a universal enrichment tool for interpreting omics data," *The Innovation*, vol. 2, no. 3, Article ID 100141, 2021.

[31] S. Hänzelmann, R. Castelo, and J. Guinney, "GSVA: gene set variation analysis for microarray and RNA-seq data," *BMC Bioinformatics*, vol. 14, no. 1, Article ID 7, 2013.

[32] L. J. Jensen, M. Kuhn, M. Stark et al., "STRING 8—a global view on proteins and their functional interactions in 630 organisms," *Nucleic Acids Research*, vol. 37, no. Suppl_1, pp. D412–D416, 2009.

[33] J. W. Newburger, M. Takahashi, M. A. Gerber et al., "Diagnosis, treatment, and long-term management of Kawasaki disease," *Circulation*, vol. 110, no. 17, pp. 2747–2771, 2004.

[34] H. Wickham, *ggplot2: Elegant Graphics for Data Analysis*, Springer International Publishing, New York, 2016.

[35] M. Koga, T. Ishihara, M. Takahashi, Y. Umezawa, and S. Furukawa, "Activation of peripheral blood monocytes and macrophages in Kawasaki disease: ultrastructural and immunocytochemical investigation," *Pathology International*, vol. 48, no. 7, pp. 512–517, 1998.

[36] Y. Pan and Q. Fan, "Identification of potential core genes in immunoglobulin-resistant Kawasaki disease using bioinformatics analysis," *Critical Reviews in Eukaryotic Gene Expression*, vol. 30, no. 1, pp. 85–91, 2020.

[37] A. A. Wolf, A. Yáñez, P. K. Barman, and H. S. Goodridge, "The ontogeny of monocyte subsets," *Frontiers in Immunology*, vol. 10, Article ID 1642, 2019.

[38] R. van Furth, Z. A. Cohn, J. G. Hirsch, J. H. Humphrey, W. G. Spector, and H. L. Langevoort, "The mononuclear phagocyte system: a new classification of macrophages,

monocytes, and their precursor cells," *Bulletin of the World Health Organization*, vol. 46, no. 6, pp. 845–852, 1972.

[39] C. Auffray, M. H. Sieweke, and F. Geissmann, "Blood monocytes: development, heterogeneity, and relationship with dendritic cells," *Annual Review of Immunology*, vol. 27, no. 1, pp. 669–692, 2009.

[40] A. J. Murphy, M. Akhtari, S. Tolani et al., "ApoE regulates hematopoietic stem cell proliferation, monocytosis, and monocyte accumulation in atherosclerotic lesions in mice," *The Journal of Clinical Investigation*, vol. 121, no. 10, pp. 4138–4149, 2011.

[41] Y. Yuan, J. Liu, Y. Zhou et al., "The relationship between monocyte-to-lymphocyte ratio and the risk of gastrointestinal system involvement in children with IgA vasculitis: a preliminary report," *Advances in Clinical and Experimental Medicine*, vol. 30, no. 10, pp. 999–1005, 2021.

[42] W. Zheng, H. Song, Z. Luo et al., "Acetylcholine ameliorates colitis by promoting IL-10 secretion of monocytic myeloid-derived suppressor cells through the nAChR/ERK pathway," *Proceedings of the National Academy of Sciences of the United States of America*, vol. 118, no. 11, Article ID e2017762118, 2021.

[43] H. Nishio, S. Kanno, S. Onoyama et al., "NOD1 ligands induce site-specific vascular inflammation," *Arteriosclerosis, Thrombosis, and Vascular Biology*, vol. 31, no. 5, pp. 1093–1099, 2011.

[44] Y. Hashimoto, R. Fukazawa, N. Nagi-Miura et al., "Interleukin-1beta inhibition attenuates vasculitis in a mouse model of Kawasaki disease," *Journal of Nippon Medical School*, vol. 86, no. 2, pp. 108–116, 2019.

[45] A. Lyu, T. A. Triplett, S. H. Nam et al., "Tumor-associated myeloid cells provide critical support for T-ALL," *Blood*, vol. 136, no. 16, pp. 1837–1850, 2020.

[46] J. Cros, N. Cagnard, K. Woollard et al., "Human $CD14^{dim}$ monocytes patrol and sense nucleic acids and viruses via TLR7 and TLR8 receptors," *Immunity*, vol. 33, no. 3, pp. 375–386, 2010.

[47] M. Lech, J. Guess, J. Duffner et al., "Circulating markers of inflammation persist in children and adults with giant aneurysms after Kawasaki disease," *Circulation: Genomic and Precision Medicine*, vol. 12, no. 4, Article ID e002433, 2019.

[48] G. Armaroli, E. Verweyen, C. Pretzer et al., "Monocyte-derived interleukin-1β as the driver of S100A12- induced sterile inflammatory activation of human coronary artery endothelial cells: implications for the pathogenesis of Kawasaki disease," *Arthritis & Rheumatology*, vol. 71, no. 5, pp. 792–804, 2019.

[49] X. B. Ling, J. L. Park, T. Carroll et al., "Plasma profiles in active systemic juvenile idiopathic arthritis: biomarkers and biological implications," *Proteomics*, vol. 10, no. 24, pp. 4415–4430, 2010.

[50] R. Reindel, S. C. Baker, K.-Y. Kim et al., "Integrins α4 and αM, collagen1A1, and matrix metalloproteinase 7 are upregulated in acute Kawasaki disease vasculopathy," *Pediatric Research*, vol. 73, no. 3, pp. 332–336, 2013.

[51] K.-U. Belge, F. Dayyani, A. Horelt et al., "The proinflammatory $D14^{+}CD16^{+}DR^{++}$ monocytes are a major source of TNF," *The Journal of Immunology*, vol. 168, no. 7, pp. 3536–3542, 2002.

[52] A. Szaflarska, M. Baj-Krzyworzeka, M. Siedlar et al., "Antitumor response of $CD14^{+}/CD16^{+}$ monocyte subpopulation," *Experimental Hematology*, vol. 32, no. 8, pp. 748–755, 2004.

[53] A. Kuroi, T. Imanishi, H. Suzuki et al., "Clinical characteristics of patients with Kawasaki disease and levels of peripheral endothelial progenitor cells and blood monocyte subpopulations," *Circulation Journal*, vol. 74, no. 12, pp. 2720–2725, 2010.

[54] I. Kwok, E. Becht, Y. Xia et al., "Combinatorial single-cell analyses of granulocyte-monocyte progenitor heterogeneity reveals an early uni-potent neutrophil progenitor," *Immunity*, vol. 53, no. 2, pp. 303–318.E5, 2020.

[55] F. Klemm, R. R. Maas, R. L. Bowman et al., "Interrogation of the microenvironmental landscape in brain tumors reveals disease-specific alterations of immune cells," *Cell*, vol. 181, no. 7, pp. 1643–1660.E17, 2020.

[56] J. C. Burns, E. V. Capparelli, J. A. Brown, J. W. Newburger, M. P. Glode, and For the US/CANADIAN KAWASAKI Syndrome Study Group, "Intravenous gamma-globulin treatment and retreatment in Kawasaki disease," *The Pediatric Infectious Disease Journal*, vol. 17, no. 12, pp. 1144–1148, 1998.

[57] A. H. Tremoulet, B. M. Best, S. Song et al., "Resistance to intravenous immunoglobulin in children with Kawasaki disease," *The Journal of Pediatrics*, vol. 153, no. 1, pp. 117–121.E3, 2008.

[58] J. M. Adrover, C. Del Fresno, G. Crainiciuc et al., "A neutrophil timer coordinates immune defense and vascular protection," *Immunity*, vol. 50, no. 2, pp. 390–402.E10, 2019.

[59] M. F. Alarcon, Z. McLaren, and H. L. Wright, "Neutrophils in the pathogenesis of rheumatoid arthritis and systemic lupus erythematosus: same foe different MO," *Frontiers in Immunology*, vol. 12, Article ID 649693, 2021.

[60] L. J. O'Neil and M. J. Kaplan, "Neutrophils in rheumatoid arthritis: breaking immune tolerance and fueling disease," *Trends in Molecular Medicine*, vol. 25, no. 3, pp. 215–227, 2019.

[61] M. Lacou, M. Leroy, N. Le Lan et al., "Muscle biopsy in anti-neutrophil cytoplasmic antibody-associated vasculitis: diagnostic yield depends on anti-neutrophil cytoplasmic antibody type, sex and neutrophil count," *Rheumatology*, vol. 60, no. 2, pp. 699–707, 2021.

[62] K. Kessenbrock, M. Krumbholz, U. Schönermarck et al., "Netting neutrophils in autoimmune small-vessel vasculitis," *Nature Medicine*, vol. 15, no. 6, pp. 623–625, 2009.

[63] L.-S. Chang, Y.-J. Lin, J.-H. Yan, M. M.-H. Guo, M.-H. Lo, and H.-C. Kuo, "Neutrophil-to-lymphocyte ratio and scoring system for predicting coronary artery lesions of Kawasaki disease," *BMC Pediatrics*, vol. 20, no. 1, Article ID 398, 2020.

[64] T. Kanai, S. Takeshita, Y. Kawamura et al., "The combination of the neutrophil-to-lymphocyte and platelet-to-lymphocyte ratios as a novel predictor of intravenous immunoglobulin resistance in patients with Kawasaki disease: a multicenter study," *Heart and Vessels*, vol. 35, no. 10, pp. 1463–1472, 2020.

[65] G. Wu, P. Yue, F. Ma, Y. Zhang, X. Zheng, and Y. Li, "Neutrophil-to-lymphocyte ratio as a biomarker for predicting the intravenous immunoglobulin-resistant Kawasaki disease," *Medicine*, vol. 99, no. 6, Article ID e18535, 2020.

[66] T.-M. Ko, J.-S. Chang, S.-P. Chen et al., "Genome-wide transcriptome analysis to further understand neutrophil activation and lncRNA transcript profiles in Kawasaki disease," *Scientific Reports*, vol. 9, no. 1, Article ID 328, 2019.

[67] K. Takahashi, T. Oharaseki, S. Naoe, M. Wakayama, and Y. Yokouchi, "Neutrophilic involvement in the damage to

coronary arteries in acute stage of Kawasaki disease," *Pediatrics International*, vol. 47, no. 3, pp. 305–310, 2005.

[68] P. Srivastava, C. Bamba, R. K. Pilania et al., "Exploration of potential biomarker genes and pathways in Kawasaki disease: an integrated in-silico approach," *Frontiers in Genetics*, vol. 13, Article ID 849834, 2022.

[69] J.-S. Kim, H. K. Kim, M. Kim et al., "Colon-targeted eNAMPT-specific peptide systems for treatment of DSS-induced acute and chronic colitis in mouse," *Antioxidants*, vol. 11, no. 12, Article ID 2376, 2022.